Pharmacological Research 217 (2025) 107805

Contents lists available at ScienceDirect

Pharmacological Research

journal homepage: www.elsevier.com/locate/yphrs

Orally effective FDA-approved protein kinase targeted covalent inhibitors (TCIs): A 2025 update

Robert Roskoski Jr

Blue Ridge Institute for Medical Research, 221 Haywood Knolls Drive, Hendersonville, NC 28791, USA

ARTICLE INFO

Keywords:
Alopecia areata
HER2-positive breast cancer
Cholangiocarcinoma
Lazertinib
Mantle cell lymphoma
Non-small cell lung cancer

Chemical compounds studied:
Acalabrutinib (PubChem CID: 71226662)
Afatinib (PubChem CID: 10184653)
Dacomitinib (PubChem CID: 11511120)
Futibatinib (PubChem CID: 71621331)
Ibrutinib (PubChem CID: 24821094)
Mobocertinib (PubChem CID: 118697832)
Neratinib (PubChem CID: 9915743)
Osimertinib (PubChem CID: 71496458)
Ritlecitinib (PubChem CID: 118115473)
Zanubrutinib (PubChem CID: 135565884)

ABSTRACT

Because aberrations of protein kinase activity play causal roles in several human diseases, this family of enzymes is one of the most important drug targets of the 21st century. Of the 88 protein kinase antagonists that are approved by the FDA, eleven of them form irreversible covalent complexes with their target enzymes. The clinical efficacy of ibrutinib, a Bruton tyrosine kinase blocker, in the treatment of mantle cell lymphoma following its 2013 approval helped to overcome a general bias against the development of irreversible drug inhibitors. Other approved targeted covalent inhibitors include acalabrutinib and zanubrutinib, which also block Bruton tyrosine kinase. Afatinib, dacomitinib, lazertinib, mobocertinib, and osimertinib inhibit members of the epidermal growth factor receptor family (ErbB1/2/3/4) and are used in the treatment of non-small cell lung cancers. Neratinib inhibits ErbB2 and is used in the management of ErbB2/HER2-positive breast cancer. Futibatinib blocks the fibroblast growth factor receptor family and is prescribed for the treatment of cholangiocarcinoma while ritlecitinib, which inhibits JAK3, is used in the management of alopecia areata. The eleven drugs considered in this review have a common mechanism of action involving the addition of a protein cysteine thiolate anion (protein—S:¯) to an acrylamide or an acrylamide-like derivative producing a thioether. The development of targeted covalent inhibitors is gaining acceptance as a valuable component of the medicinal chemist's toolbox and has made a significant impact on the development of protein kinase antagonists and receptor modulators.

1. Targeted covalent inhibitors including protein kinase antagonists

Because of genetic alterations and overexpression including mutations and translocations, the dysregulation of protein kinase activity is involved in the pathogenesis of many diseases including cardiovascular, inflammatory, nervous, and autoimmune diseases as well as cancer. Consequently, the protein kinase superfamily is one of the most important drug targets in the 21st century [1,2]. The pursuit of orally effective therapeutic protein kinase inhibitors was motivated in large part by the success that imatinib demonstrated in the management of Philadelphia chromosome-positive chronic myelogenous leukemia, which led to its FDA approval in 2001 [3]. This result was achieved owing to the inhibition of the activated chimeric BCR-Abl protein-tyrosine kinase (the principal biochemical lesion that causes these leukemias) by imatinib.

More than 400 protein kinase inhibitors are under clinical investigation worldwide [4,5]. Furthermore, there are 88 FDA-approved protein kinase blockers that target about two dozen different enzymes (Supplementary material). However, the current targets represent a small fraction of the protein kinase superfamily and many other protein kinases are potential therapeutic entities. Although the medical community was rather cautious in developing irreversible covalent drugs for the management of diseases, the success of ibrutinib in the treatment of mantle cell lymphomas stimulated interest in the development of targeted covalent protein kinase inhibitors [6].

Manning et al. found that the human protein kinome consists of 518 members including 478 typical and 40 atypical enzymes [7]. These

Abbreviations: AS, activation segment; BP, back pocket; BTK, Bruton protein-tyrosine kinase; C-spine, catalytic spine; CS1, catalytic spine residue 1; CL, catalytic loop; CLL, chronic lymphocytic leukemia; EGFR, epidermal growth factor receptor; ErbB, erythroblastosis related proto-oncogene of the EGFR family; F, front pocket; FGFR, fibroblast growth factor receptor; GK, gatekeeper; GRL, glycine-rich loop; JAK, Janus kinase; KLIFS-3, kinase-ligand interaction fingerprint and structure residue-3; HER2, human epidermal growth factor receptor-2; NSCLC, non-small cell lung cancer; PKA, protein kinase A; R-spine, regulatory spine; RS1, regulatory spine residue 1; Sh2, shell residue 2; STAT, signal transducer and activator of transcription; TCIs, targeted covalent inhibitors.

E-mail address: rrj@brimr.org.

https://doi.org/10.1016/j.phrs.2025.107805
Received 27 May 2025; Received in revised form 28 May 2025; Accepted 28 May 2025
Available online 30 May 2025

proteins mediate the following reaction;

$$MgATP^{1-} + protein\text{–}O{:}H \rightarrow protein\text{–}O{:}PO_3^{2-} + MgADP + H^+$$

Note that the phosphorylium ion ($:PO_3^{2-}$) and not the phosphate ($:OPO_3^{2-}$) group is transferred from ATP to the protein substrate. Based upon the nature of the phosphorylated –OH groups, these enzymes are classified as protein-tyrosine kinases (90 members), protein-tyrosine-kinase–like enzymes (43), and protein-serine/threonine kinases (385). The protein-tyrosine kinases consist of both receptor (58) and non-receptor (32) enzymes. A small group of kinases including MEK1/2 catalyze the phosphorylation of threonine and then tyrosine residues within the activation loop of their target protein kinases; these are classified as dual specificity kinases. Assuming a human genome complement of 20,000 genes and a human kinome of about 500 genes, then protein kinases represent about 2.5 % of all genes. Manning et al. reported that 244 protein kinases map to cancer amplicons or to disease loci [7] so that we can expect an increase in the number of therapeutic protein kinases that will be targeted for the treatment of additional diseases [8].

Drugs that form irreversible covalent adducts with proteins were disfavored owing to toxicity and safety concerns [9]. Aspirin, however, is a TCI that has been in the therapeutic armamentarium since 1899. Roth et al. and Botting et al. reported that aspirin exerts its therapeutic effect in humans by acetylating serine 530 of cyclooxygenase-1 [10,11]. Moreover, irreversible proton pump antagonists that decrease stomach acid production such as esomeprazole, omeprazole, and lansoprazole are safe, effective, and widely used in the treatment of dyspepsia and gastroesophageal reflux [9]. That these three over-the-counter medicines are available without a prescription indicates their measure of safety. These agents react with a gastric proton pump (H^+/K^+ ATPase) cysteine to form an inactive product [12]. Furthermore, rasagiline and selegiline, which are FDA approved for the treatment of Parkinson disease, represent additional examples of irreversible enzyme inhibitors [13]. These acetylenic drugs, which inhibit type B monoamine oxidase by forming a covalent complex with the N5 of its FAD cofactor, are prescribed as a monotherapy in the management of early Parkinsonism or as an adjunct therapy in advanced Parkinsonism [14]. The US FDA has approved 45 drugs that form covalent bonds with their target protein since 2001 and fourteen drugs with this mechanism of action were approved in the past decade [6].

Of the 88 small molecule protein kinase inhibitors approved by the FDA as of May 2025, eleven of these drugs form a covalent bond with their target protein [15,16]. The eleven targeted covalent inhibitors (TCIs) of protein kinases include afatinib, dacomitinib, lazertinib, mobocertinib, osimertinib (all five directed toward EGFR in NSCLC), neratinib (targeting ErbB2 in HER2-positive breast cancers), acalabrutinib (directed toward BTK in mantle cell lymphomas, chronic lymphoblastic leukemias, and small cell lymphomas), ibrutinib (targeting BTK in mantle cell lymphomas, marginal zone lymphomas, chronic graft vs. host disease, chronic lymphocytic leukemias, and Waldenström macroglobulinemia), zanubrutinib (directed toward BTK in mantle cell lymphomas), futibatinib (targeting FGFR2 in patients with cholangiocarcinomas with FGFR2 gene fusions or rearrangements), and ritlecitinib (directed toward JAK3 in patients with alopecia areata). Note that EGFR, ErbB2/HER2, and FGFR2 are transmembrane receptor tyrosyl kinases and BTK and JAK3 are nonreceptor protein-tyrosine kinases. According to Singh et al. [9], a TCI is “an inhibitor bearing a bond-forming functional group of low reactivity that, following binding to the target protein, is positioned to react rapidly with a specific non-catalytic residue at the target site.”

2. An overview of protein kinases

2.1. The EGFR family and their ligands

The EGFR protein-tyrosine kinases (ErbB1/2/3/4) and their downstream protein cascades are among the most studied signal transduction modules in biology [17]. Stanley Cohen initiated the course of study when he isolated the epidermal growth factor (EGF), its receptor (EGFR), and described its many biochemical activities [18]. He discovered that EGFR exhibited protein-tyrosine kinase activity, which was unknown at the time, and not the well-known protein-serine/threonine kinase activity exhibited by PKA (see Ref. [19] for a historical review). Cohen et al. demonstrated that a single 170-kDa polypeptide chain bound EGF and catalyzed protein phosphorylation [20]. Furthermore, EGFR was the first receptor that linked gene mutations and protein overexpression with cancer [21]. This receptor protein-tyrosine kinase family and its downstream components are among the most studied signal transduction modules owing to their roles in the pathogenesis of malignancies [22–25].

The human epidermal growth factor receptor (HER) lineage consists of four members that belong to the ErbB family of proteins (ErbB1/2/3/4) [23]. The *ERBB* gene nomenclature was derived from the related avian viral erythroblastosis oncogene. The four constituents of this receptor gene lineage include: (i) *EGFR/ERBB1/HER1,* (ii) *ERBB2/-HER2/NEU*, (iii) *ERBB3/HER3,* and (iv) *ERBB4/HER4.* Although there is wide variation, the ErbB nomenclature is used in the biological sciences while the HER nomenclature is used in clinical studies and reports. Schechter et al. reported that several rat neuro/glioblastomas contain the *Neu* oncogene, which is related to the rat *Erbb2* gene of the EGFR family [26]. This result argued for the putative role of the ErbB family in the pathogenesis of various neoplasms, which led to the use of *NEU* in human gene nomenclature. The ErbB family of receptors is universally expressed in mesenchymal, epithelial, and neuronal cells as well as their undifferentiated precursors.

Based upon the amino acid sequence of EGFR as determined by cDNA analysis, Ulrich et al. proposed that this protein consists of an extracellular ligand binding domain, a hydrophobic transmembrane segment, and an intracellular protein kinase domain [27]. This prescient hypothesis applies to nearly all receptor protein-tyrosine kinases. The EGFR protein kinase family members possess an extracellular portion containing four parts: domains I and III are related leucine-rich ligand binding sections and domains II and IV are cysteine-rich sections that contain about a dozen disulfide bonds [22–25]. Moreover, the second segment participates in both homo and heterodimer formation with EGFR family members, which is necessary for the activation of their protein kinase activity [23,24]. The extracellular portion precedes a single transmembrane segment containing 20–26 amino acid residues and this is followed by an intracellular section containing about 550 amino acid residues that consists of (i) a small juxtamembrane segment, (ii) a catalytic protein kinase entity, and (iii) an extensive C-terminal tail (Fig. 1).

The ligands that bind to each of the ErbB proteins are enumerated in Fig. 1. The ErbB3 receptor is kinase impaired as indicated by the stop sign. Like other receptor protein-tyrosine kinases, the EGFR family consists of functional dimers or higher oligomers [17]. There is a single isoform of ErbB1, two ErbB2 isoforms that differ owing to alternative mRNA splicing, and two ErbB3 isoforms, one of which is missing residues 1–59. Increasing the complexity of the EGFR family, there are two different extracellular juxtamembrane versions (JMa and JMb) of ErbB4 and two different versions of the C-terminal tail (CTa and CTb) of this receptor. Accordingly, there are four ErbB4 isoforms that result from alternative splicing: JMaCTa, JMaCTb, JMbCTa, and JMbCTb. Experiments indicate that ErbB2 is the preferred dimerization partner for the other ErbB family members [28,29]. Moreover, Pinkas-Kramarski et al. reported that ErbB2 in combination with ErbB1 or with ErbB3 possess robust signaling activity [30]. That the heterodimer of ErbB2 (which

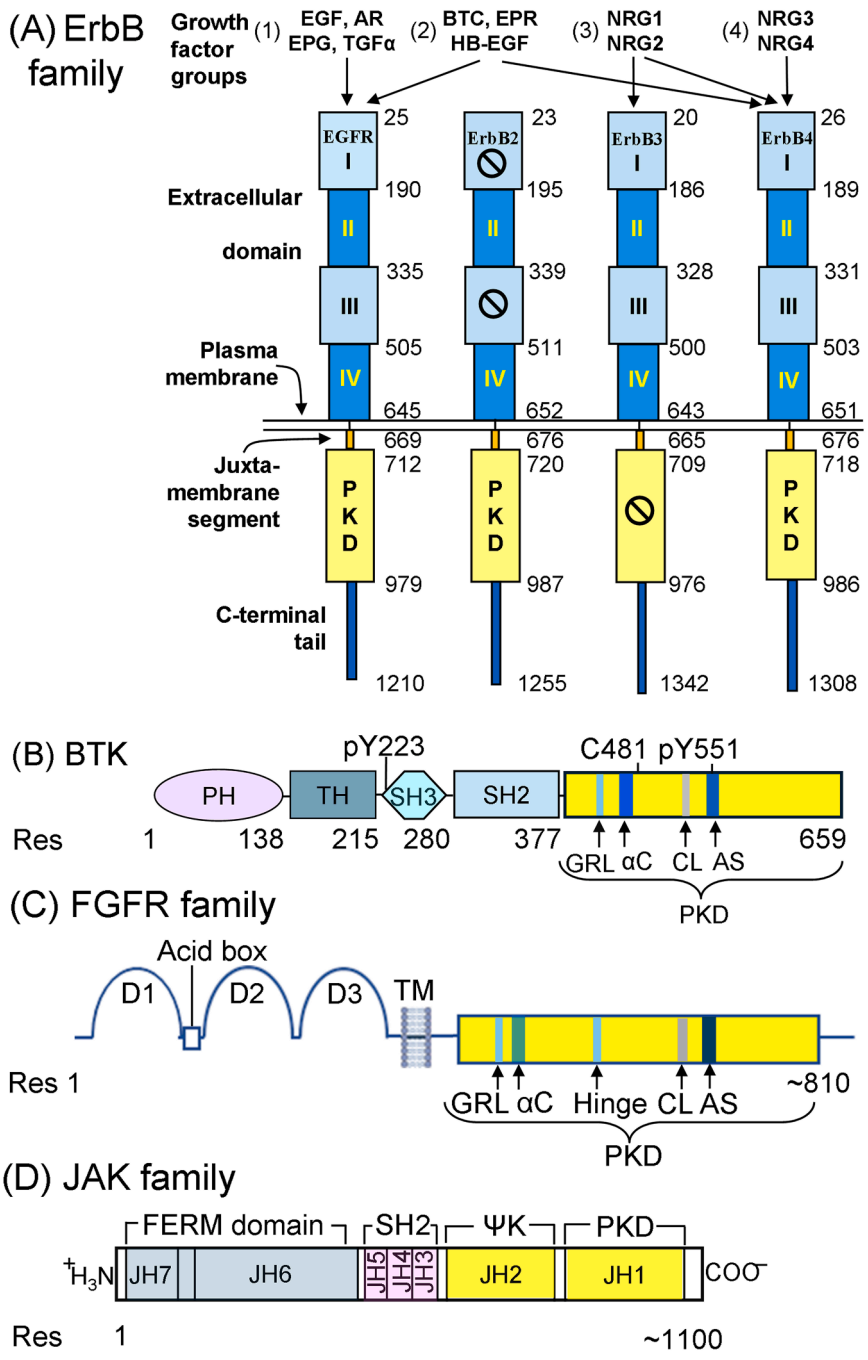

Fig. 1. (A) Organization of the human epidermal growth factor receptor family members consisting of EGFR/ErbB1/HER1, ErbB2/HER2/NEU, ErbB3/HER3 and ErbB4/HER4. The extracellular component of each receptor consists of four domains (I–IV). Domains I and III participate in ligand binding (except for those of ErbB2/HER2, which are marked with the stop symbol), and domain II participates in homo or heterodimer formation. The ErbB3/HER3 protein kinase domain, which is marked with the stop symbol, is catalytically impaired. The numbers represent amino acid residues of the nascent protein including the signal peptide (which is not depicted); each number corresponds to the initial residue of the adjacent segment except for (i) the last residues of the extracellular domains and (ii) the end of the proteins. The growth factor groups (1–4) that bind to the receptors are indicated. EGF, epidermal growth factor; AR, amphiregulin; EPG, epigen; TGFα, transforming growth factor-α; BTC, betacellulin; EPR, epiregulin; HB-EGF, heparin-binding epidermal growth-like factor; Nrg-1/2/3/4, neuregulin-1/2/3/4. (B) Organization of BTK (Bruton protein-tyrosine kinase). The relative size of each segment is indicated by the amino acid residue number given below the diagram. Acalabrutinib binds covalently with C481. (C) Organization of the FGFR family. (D) Organization of the JAK family kinases. AS, activation segment; CL, catalytic loop; PKD, protein kinase domain; PH, pleckstrin homology domain; pY, phosphotyrosine; ΨK, pseudokinase; TH, TEC homology domain; TM, transmembrane.

does not bind a growth factor) and ErbB3 (which lacks protein kinase activity) exhibits robust signaling activity is paradoxical.

2.2. *Structures of the small and large lobes and the protein kinase fold*

The protein kinase catalytic domains contain ≈ 250–300 amino acid residues. Like other protein kinases, the EGFR protein kinase domain has a small N-terminal lobe and large C-terminal lobe (Fig. 2 A) as first reported for PKA by Knighton et al. (PDB ID: 2cpk) [31]. The small and large lobes form a cleft that binds ATP. The N-terminal lobe contains a flexible conserved glycine-rich loop (GRL) or ATP-phosphate–binding loop (P-loop), which is near the phosphates of the ATP substrate. The

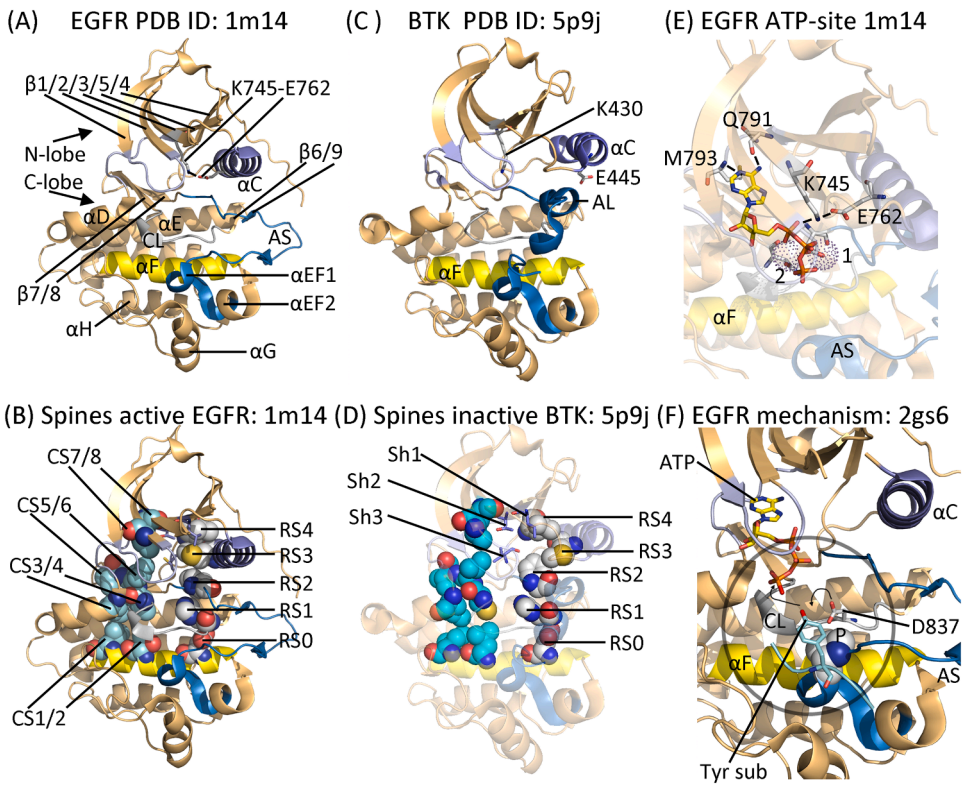

Fig. 2. (A) Active EGFR and its spine residues (B). (C) Inactive BTK and its spine residues (D). (E) Model of the ATP-binding site of EGFR. (F) Catalytic mechanism of action of EGFR. The chemistry occurs within the circle. AS, activation segment; CL, catalytic loop. P refers to P877, which serves as a platform for the protein-tyrosine substrate (Tyr sub). Figs. 2, 3, and 7 were prepared using the PyMOL Molecular Graphics System Version 2.5.4 Schrödinger, LLC.

GRL contains a GxGxΦG signature where Φ refers to a hydrophobic residue and is phenylalanine in EGFR. The GRL, which connects the β1- and β2-strands, covers the ATP-binding site. The β1- and β2-strands of the N-terminal lobe interact with the adenine portion of ATP and they engage with small molecule inhibitors including those listed in Table 1. The β3-strand contains a canonical Ala-Xxx-Lys signature, the lysine of which in human EGFR (K645) forms an electrostatic bond with a conserved glutamate that occurs near the center of the αC-helix (E762) (Fig. 2 A). The formation of an electrostatic bond involving the β3-strand lysine and the αC-helix glutamate is required for the generation of an active enzyme conformation and this structure corresponds to the "αC_{in}" conformation. In comparison, this salt bridge is lacking in many inactive forms of protein kinases and such structures correspond to an inactive "αC_{out}" conformation as depicted for BTK (Fig. 2 C). The αC_{in} structure is necessary, but not sufficient, for the expression of maximal enzyme activity.

The carboxyterminal lobe contains a mobile activation segment (AS) or activation loop (AL) with an unfolded or open conformation in active enzymes (Fig. 2 A) and a closed conformation in inactive enzymes (Fig. 2 C). The activation segment begins with a conserved DFG (Asp-Phe-Gly) signature. The DF pair displays two different conformations. In the active state, the aspartate side chain carboxylate moiety extends toward the ATP-binding pocket and coordinates Mg^{2+}. This structure corresponds to the "DFG-D_{in}" conformation. In a dormant activation segment structure, the aspartate carboxylate of the DFG sequence points away from the active site in the "DFG-D_{out}" conformation. The ability (DFG-D_{in}) or inability (DFG-D_{out}) of the DFG-aspartate to bind to Mg^{2+} in the active site is the important difference. See Ref. [1] for an overview of the two activation segment conformations. Although the activation segment of protein kinases including the FGFR family and the JAK family most often ends with APE (Ala-Pro-Glu), this segment ends with SPE in BTK and ALE (Ala-Leu-Glu) in the ErbB family. The last eight residues of the four ErbB family activation segments are made up of PIKWMALE and this octet forms the protein-substrate positioning loop. The R-group of proline in this sequence functions as a platform that supports the tyrosyl residue of the protein substrate that is phosphorylated (Fig. 2F) [32]. Although the activation segment of the EGFR family contains a tyrosine residue that can be phosphorylated, unlike many other protein kinases, this phosphorylation is not required for enzyme activation but it is required for signal transduction [33].

ErbB1/2/4 are functional protein-tyrosine kinases that occur in active and inactive conformations [23]. In comparison, ErbB3 lacks a critical catalytic residue and is thus enzymatically inactive. Furthermore, it assumes the conformation of an inactive protein kinase. The C-terminal lobe of protein kinases is mainly α-helical with eight conserved segments (αD–αI and αEF1/2). The first protein kinase X-ray crystal structure (PKA) exhibited two short helices proximal to the large lobe αF-helix, which were unnamed at the time (PDB ID: 2cpk) [31]. However, the αEF1/2 helices occur in all active protein kinases and they represent a seventh and eighth conserved helix in the carboxyterminal lobe (Fig. 2 A). The activation segment of active EGFR is open and extends outward while that of dormant BTK is closed and more compact (Fig. 2 A/C) [25]. The large lobe of active protein kinases contains four short β-strands (β6-β9) (Fig. 2 A). The β6-strand, which is proximal to the catalytic loop, interacts with the β9-strand of the activation segment. The β7-strand is located between the catalytic loop and the activation segment and it interacts with the adjacent distal β8-strand. The inactive forms of all four EGFR family members contain the β7- and β8-strands, but they lack the β6- and β9-strands. The important residues of the EGFR family, the FGFR family, BTK, and JAK3 are provided in Table 2.

2.3. Structures of the hydrophobic spines in active and in dormant protein kinase domains

2.3.1. The regulatory spine

Kornev et al. [34,35] examined the tertiary structures of functional

Table 1
Orally effective FDA-approved irreversible small molecule protein-tyrosine kinase inhibitors and their therapeutic indications.

Drug (Code) Trade name	Year approved	Primary targets[a]	Therapeutic indications[b]
Afatinib (BIBW 2992) Tovok	2013	ErbB1/2/4	Mutant *EGFR* NSCLC
Dacomitinib (PF002999804) Visimpro	2018	ErbB1/2/4	Mutant *EGFR* NSCLC
Lazertinib (GNS1480), Lazcluze	2024	EGFR	NSCLC with ex19 del or ex21 L858R substitutions with amivantamab
Mobocertinib (TAK−788) Exkivity	2021	EGFR	NSCLC with *EGFR*-positive exon 20 insertions
Osimertinib (AZD−9292) Tagrisso	2015	EGFR T970M	Mutant *EGFR* NSCLC
Neratinib (HKI−272) Nerlynx	2017	HER2	HER2-positive breast cancer
Acalabrutinib (ACP−196) Calquence	2017	BTK	Mantle cell lymphoma; CLL; SLL
Ibrutinib (PCI−32765) Imbruvica	2013	BTK	CLL; graft vs. host disease; mantle cell lymphoma; marginal zone lymphoma; SLL; Waldenström macroglobulinemia
Zanubrutinib (BGB3111) Brukinsa	2019	BTK	Mantle cell lymphoma
Futibatinib (TAS−120) Lytgobi	2022	FGFR1/2/3/4	Cholangiocarcinomas with FGFR2 fusion proteins or other rearrangements
Ritlecitinib (PF−06651600) Litfulo	2023	JAK3	Alopecia areata

[a] Although some of these drugs are multikinase inhibitors, only the primary therapeutic targets are given here.
[b] CLL, chronic lymphocytic leukemia; NSCLC, non-small cell lung cancer; SLL, small lymphocytic lymphoma.

and dormant structures of about two dozen protein kinases and they found a group of catalytically important residues by a local spatial pattern (LSP) alignment protocol. The residues that constitute the catalytic and regulatory spines were determined by their three-dimensional location based upon X-ray crystal structures and not by an amino acid signature such as HRD or DFG. Their structural studies revealed a supporting framework of eight hydrophobic residues that form a catalytic or C-spine and four hydrophobic residues that form a regulatory or R-spine (Fig. 2B/D). The R-spine contains a residue from the αC-helix and another from the activation segment, whose structures are pivotal in determining functional and dormant states. The C-spine facilitates ATP binding and thereby mediates catalysis. The correct configuration of both spines is required for the generation of an active enzyme.

The regulatory spine consists of a residue from the beginning of the β4-strand (L777 for EGFR), from the carboxyterminal end of the αC-helix (M766), DFG-F856, along with HRD-H835 of the catalytic loop. M766 and comparable residues from other protein kinases are four residues carboxyterminal to the conserved αC-glutamate [25]. The backbone N–H of RS1 (H835 in EGFR) is secured to the αF-helix by a hydrogen bond to a side chain carboxyl group of a canonical aspartate residue (D872). The activation loop, the protein-substrate positioning loop, and the αHI loop of protein kinase domains, including the ErbB/HER family, interact hydrophobically with the αF-helix [34,35].

2.3.2. *The catalytic spine*

The catalytic spine of protein kinases contains residues from the N-terminal and C-terminal lobes as well as the ATP adenine [35,36]. The two residues from the N-terminal lobe of EGFR that interact with the adenine group of ATP include V726 (CS7) near the origin of the β2-strand and A743 (CS8) from the conserved β3-strand Ala-Xxx-Lys. Furthermore, L844 (CS6) from the middle of the β7-strand of the C-terminal lobe binds to the ATP adenine of the active enzyme. V726 (CS7), A743 (CS8), and L844 (CS6) usually make hydrophobic contact with the pharmacophores of ATP-competitive inhibitors and TCIs. V843 (CS4) and V845 (CS5), which are next to L844, interact with L798 (CS3) at the beginning of the αD-helix. L798 (CS3) interacts hydrophobically with L907 (CS1) and V843 (CS4) interacts hydrophobically with T903 (CS2) in the αF-helix. Note that both spines are anchored to the αF-helix,

Table 2
Important amino acid residues in selected human protein-tyrosine kinases.

	EGFR	ErbB2	ErbB3	ErbB4	BTK	FGFR1	FGFR2	FGFR3	FGFR4	JAK3	Functions
Number of residues	1210	1255	1342	1308	659	822	821	806	802	1124	
Signal peptide	1–24	1–22	1–19	1–25	None	1–21	1–21	1–22	1–21	None	
Extracellular segment	25–645	23–652	20–643	26–651	None	22–376	22–377	23–375	22–379	None	Ligand binding
Transmembrane segment	646–668	653–675	644–664	652–675	None	377–397	378–398	376–396	370–390	None	
Intracellular portion	669–1210	676–1255	665–1342	676–1308	1–659	398–822	399–821	397–806	391–802	1-1124	Catalysis and signaling
Protein kinase domain	712–979	720–987	709–966	718–985	402–655	478–767	481–770	472–761	467–755	822–1111	Catalyzes substrate phosphorylation
The β3-*K* of *K*/E/D/D	K745	K753	K742	K751	K430	K514	K517	K508	K503	K855	Anchors ATP α- and β-phosphates
αC-*E* of K/*E*/D/D	E762	E770	H759	E768	E445	E531	E534	E525	E520	E871	Forms salt bridge with β3-lysine
Gatekeeper residue	T790	T798	T787	T796	T474	V561	V564	V555	V550	M902	Regulates access to back pocket
Catalytic HR*D* residue, the first *D* of K/E/*D*/D	837	845	N834	843	521	623	626	617	612	949	Catalytic base (abstracts proton)
Catalytic loop *N* (HRD $(x)_4$*N*	842	850	839	848	526	628	631	622	617	954	Chelates Mg^{2+}(2)
AS[a] DFG, the second *D* of K/E/D/*D*	855	863	852	861	539	641	644	635	630	967	Chelates Mg^{2+}(1)
AS[a] phosphorylation sites	Y869	Y877	Y868	Y875	Y551	Y653/4	Y656/7	Y647/8	Y642/3	Y980/1	Stabilizes activation segment
Molecular weight (kDa)	134	138	148	147	76.3	91.9	92.0	87.7	87.9	125	
UniProtKB ID	P00533	P04626	P21860	Q15303	Q06187	P11362	P21802	P22607	P22455	P52333	

[a]AS, activation segment.

a very hydrophobic component that is entirely within the protein. The core αF-helix buttresses both spines and they, in turn, secure the protein kinase catalytic residues. See Table 3 for a list of the residues of the spines of human ErbB1/2/3/4, BTK, FGFR1/2/3/4, and JAK3.

The protein kinase spines play a crucial role in the structure and function of these enzymes and we are unable to overemphasize their importance in the functioning of the protein kinase superfamily as well as their interactions with small molecule kinase inhibitors. For a listing of spine residues in various protein kinases, see Refs. [22–25] for the EGFR family of protein-tyrosine kinases, Ref. [37] for the Bruton non-receptor protein-tyrosine kinase, Ref. [38] for the fibroblast growth factor receptor protein-tyrosine kinase family, Ref. [39] for the Janus kinase (JAK) nonreceptor protein-tyrosine kinase family, Refs. [40,41] for the ALK pleotrophin and midkine receptor protein-tyrosine kinase, Ref. [42] for the Kit stem cell receptor protein-tyrosine kinase, Ref. [43] for the MET hepatocyte growth factor receptor protein-tyrosine kinase, Ref. [44] for the PDGFRα/β protein-tyrosine kinases, Ref. [45] for the RET glial-cell derived receptor protein-tyrosine kinase, Ref. [46] for the VEGFR1/2/3 protein-tyrosine kinase family, Ref. [47] for the ROS1 orphan receptor protein-tyrosine kinase, Refs. [48,49] for the Src non-receptor protein-tyrosine kinase, Refs. [50,51] for the MEK1/2 dual specificity protein kinases, Refs. [52,53] for the ERK1/2 protein-serine/threonine kinases, Refs. [36,54] for the cyclin-dependent protein-serine/threonine kinases, and Refs. [55,56] for the RAF protein-serine/threonine kinases.

2.3.3. The gatekeeper and other shell residues

Stemming from site-directed mutagenesis experiments, Meharena et al. found three residues in protein kinase A (PKA) that stabilize the R-spine which they named shell residues [57]. These authors called the R-spine residues RS0, RS1, RS2, RS3, and RS4 as they went from the αF-helix aspartate to the β4-strand at the top of the regulatory spine (Fig. 2B). They designated the three shell residues as Sh1, Sh2, and Sh3 where Sh2 is the classical gatekeeper residue. The term gatekeeper denotes the function of these residues in regulating the entry of the ligand into a hydrophobic back pocket next to the adenine binding site [58,59] that is occupied by components of many small molecule protein kinase inhibitors. Using their local spatial alignment results, Meharena et al. found that only three of 14 amino acid residues adjacent to RS3 and RS4 of PKA are maintained and they reported that shell residues promote R-spine stabilization [57]. A comparison of the regulatory spines of active EGFR and those of inactive BTK demonstrates that RS3 of the inactive enzyme is displaced outward when compared with active EGFR, a result that is consistent with the idea that the αC-helix is displaced outward in dormant BTK (Fig. 2).

2.3.4. The binding pocket for ATP and small molecule inhibitors

The hinge-linker residues connect the amino-terminal lobe to the carboxyterminal lobe [25]. The 6-amino group of ATP characteristically forms a hydrogen bond with the backbone carbonyl group of the first hinge residue; in EGFR it hydrogen bonds with the carbonyl oxygen of Q791 (PDB ID: 2GS6). The *N*1 nitrogen of adenine hydrogen bonds with the –NH group of M793, the third hinge residue. The α-phosphate group of ATP binds to AxK-K745 of the β3-strand, which in turn makes a salt bridge with the αC-helix E762 (Fig. 2E). Moreover, the ATP γ-phosphoryl group forms an electrostatic bond with Mg^{2+}(1), which in turn binds to DFG-D854 (not shown). Crystallographic studies show that the adenine group extends to the β2-strand, but not to the β3-strand. In contrast, most low molecular weight steady-state ATP-competitive inhibitors extend to the β3-strand and many extend even further toward the αC-helix into the back pocket.

2.3.5. The catalytic loop and activation segment

Active protein kinases contain an amino acid signature made up of K/E/D/D (Lys/Glu/Asp/Asp) and these residues play essential structural and mechanistic roles (Table 2) [41]. The EGFR β3-strand K745 is the first residue of this signature and it forms a salt bridge with the second residue of this signature (αC-helix E762) [25]. The catalytic loop contains eight residues with a conserved HRD(x)$_4$N signature; the HRD-*D* residue is the first *D* of K/E/*D*/D. This loop consists of an HRDLAARN sequence in most receptor protein-tyrosine kinases including ErbB1/2/4 and FGFR1/2/3/4. On the other hand, catalytically deficient ErbB3 contains HR*N*LAARN with an asparagine (*N*) replacing aspartate (D). The catalytic aspartate (HRD-D837) of EGFR serves as a Lowry-Brönsted base that abstracts a proton from the protein substrate tyrosyl –OH group (Fig. 2 F). Zhou and Adams suggested that the catalytic loop protein kinase aspartate positions the substrate –OH group for an in-line nucleophilic attack [60]. Additional experiments show that the DFG-D855 of protein kinases at the beginning of the activation segment binds Mg^{2+} (1) while the distal catalytic loop asparagine (N842) coordinates a second Mg^{2+}(2) as depicted in Fig. 2E. The activation loop DFG-*D* is the second *D* of the K/E/D/*D* signature.

2.4. Bruton protein-tyrosine kinase (BTK)

BTK was recognized as a nonreceptor protein-tyrosine kinase in 1993; a deficiency of this gene product is found in patients with X-linked agammaglobulinemia [61–64]. Individuals with this disorder display

Table 3
Spine and shell residues in selected protein-tyrosine kinases[a].

		KLIFS No[a]	ErbB1	ErbB2	ErbB3	ErbB4	BTK	FGFR1	FGFR2	FGFR3	FGFR4	JAK3
Regulatory spine												
β4-strand (N-lobe)	RS4	38	L777	L785	L774	L783	L460	L547	L550	L541	L536	Y886
C-helix (N-lobe)	RS3	28	M766	M774	I763	M772	M449	M535	M538	M529	M524	L875
Activation loop (C-lobe) F of DFG	RS2	82	F856	F864	F853	F862	F540	F642	F645	F636	F631	F968
Catalytic loop His (C-lobe)	RS1	68	H835	H843	H832	H841	H519	H621	H624	H615	H610	H947
F-helix (C-lobe)	RS0	None	D896	D904	D893	D902	D579	D682	D685	D676	D671	D1009
R-shell												
Two residues upstream from the gatekeeper	Sh3	43	L788	L796	L785	L784	I472	V559	V562	V553	V548	L900
Gatekeeper, end of β5-strand	Sh2	45	T790	T798	T787	T796	T474	V561	V564	V555	V550	M902
αC-β4 loop	Sh1	36	C775	S783	V772	V781	V458	I545	I548	I539	I534	V884
Catalytic spine												
β3-AxK motif (N-lobe)	CS8	15	A743	A751	C740	A749	V416	A512	A515	A506	A501	V863
β2-strand (N-lobe)	CS7	11	V726	V734	V723	V732	A428	V492	V495	V486	V481	A853
β7-strand (C-lobe)	CS6	77	L844	L852	L841	L850	L528	L630	L633	L624	L619	L956
β7-strand (C-lobe)	CS5	78	V845	V853	V842	V851	V529	V631	V634	V625	V620	V957
β7-strand (C-lobe)	CS4	76	V843	V851	V840	V849	C527	V629	V632	V623	V618	I955
D-helix (C-lobe)	CS3	53	L798	L806	L795	L804	L482	L569	L572	L563	L558	L910
F-helix (C-lobe)	CS2	None	T903	T911	T900	T909	L586	L689	L692	L683	L678	V1016
F-helix (C-lobe)	CS1	None	L907	L915	L904	L913	I590	I693	I696	I687	I682	L1020

[a] From Refs. [34–36], https://klifs.net/, and https://www.uniprot.org/uniprotkb/.

alterations in B cell function and this characteristic is in agreement with the restriction of clinical features to B cell immunity. The Lyn and Syk protein kinases of the Src family are upstream of BTK while phospholipase γ2 is downstream in the BTK signaling cascade leading to the production of diacylglycerol and inositol trisphosphate [48]. The former activates protein kinase C and the latter leads to the release of Ca^{+2} from the endoplasmic reticulum. BTK belongs to the TEC family of protein-tyrosine kinases including BTK, BMX (bone marrow-expressed kinase), ITK (inducible T cell kinase), TXK (also known as RLK, resting lymphocyte kinase), and TEC [7]. TEC (T-helper cell) kinase participates in immune responses. BTK contains a short amino-terminal pleckstrin homology (PH) domain, followed by a TEC homology (TH) domain, an SH3 domain, an SH2 domain, and finally a C-terminal protein kinase domain (Fig. 1B); these components are found in the other members of the TEC family of protein kinases.

Like the EGFR family, BTK contain a glycine-rich loop (GRL) with a GxGxΦG signature (^{409}GTGQFG^{414}) [37]. Φ refers to a hydrophobic residue and is phenylalanine in BTK, the ErbB family, the FGFR family, and JAK3. Owing to their role in ATP binding and ADP release, the glycine-rich loops are pliant. As described for other protein kinases, BTK contains a conserved β3-strand Ala-Xxx-Lys (^{428}AIK^{430}) sequence and an αC-helix glutamate (E445) that forms an electrostatic bond with a conserved β3-strand lysine in the active enzyme conformation. BTK contains the conserved ^{519}HRDLAARN^{526} sequence at the beginning of the catalytic loop. It also contains the conserved ^{539}DFG^{541} signature at the beginning of the activation segment and a ^{565}PPE^{567} sequence at the end of the activation segment.

All protein kinases including BTK have a small amino-terminal lobe and large carboxyterminal lobe [1] (Fig. 2 C). Although both lobes participate in ATP binding, the small lobe plays a major role in this process. The BTK K430 ε-amino group forms an electrostatic bond with the αC-helix E445 carboxylate group (the *E* of K/*E*/D/D) that stabilizes their interactions with the ATP phosphates [37]. The salt bridge involving the β3-lysine and the αC-glutamate is required for the formation of an active "αC-in" protein kinase conformation. On the other hand, E445 and K430 of the inactive enzyme fail to interact and this corresponds to an "αC-out" conformation (Fig. 2 C). The important residues of BTK are given in Table 2 and the spine and shell residues are provided in Table 3.

2.5. Fibroblast growth factors and their receptors

The human fibroblast growth factor (FGF) family is made up of 22 members [65]. Although these are identified as FGF1–23, factors 15 and 19 represent the same molecule giving 22 total factors. With the exception of FGF11/12/13/14, the remaining factors are glycoproteins that are secreted by exocytosis from the cell of origin and they interact with the transmembrane fibroblast growth factor receptors (FGFRs). A total of 18 of these factors are receptor ligands. The intracellular growth factors (FGF11/12/13/14) interact with voltage-gated sodium channels. The FGFs range in size from 155 residues (FGF1) to 288 residues (FGF2). The FGFs contain a core domain with about 120 amino acid residues that assume a globular structure that makes 12 β-strands arranged into three groups of four-stranded β-sheets [66]. This core domain is bordered by differing N-terminal and C-terminal sequences that account for the specificity and selectivity of the growth factors.

The FGFRs consist of an extracellular portion containing three immunoglobulin-like domains (D1/2/3), a transmembrane (TM) segment, and an intracellular protein-tyrosine kinase domain (PKD) (Fig. 1) [66]. An acid box containing a short stretch of glutamates and aspartates is found between D1 and D2. FGFs bind to the region of the extracellular segment involving D2, D3, and the D2-D3 linker. Ligand-binding specificity of FGFR1/2/3 is regulated in part by alternative splicing in the D3 domain of these receptors. The amino-terminal segment of D3 is encoded by exon IIIa and the carboxyterminal portion of D3 is encoded by one of two mutually exclusive exons (exon IIIb or exon IIIc) where III refers to D3. Experiments indicate that alternative splicing changes the sequence of key ligand-interacting residues to confer FGF binding specificity. Such alternative splicing is cell and tissue specific. FGFR4 mRNA fails to undergo alternative splicing of the encoded D3 domains.

The binding of the FGFs to their receptors produces receptor dimerization, transphosphorylation, and subsequent protein kinase activation [17]. Six tyrosine residues of FGFR1 are sequentially phosphorylated to produce the fully activated enzyme [67]. Downstream signaling by the FGFRs resembles that of most other receptor protein-tyrosine kinases including EGFR/ErbB1/2/3/4. All four FGFRs result in the activation of the Ras-Raf-MEK-Erk Map kinase signaling cascade that regulates cell growth, cell division, and differentiation and the PI3K/Akt module that regulates cell survival [66,68]. The activated receptors also promote activation of phospholipase C and the generation of inositol-trisphosphate and diacylglycerol, which stimulate cell migration. The four enzymes also activate the STAT (signal transducer and activator of transcription) pathway leading to the transcription of numerous genes.

2.6. Janus kinases

The Janus kinases are large intracellular proteins containing about 1100 amino acid residues. They possess seven JAK homology modules labeled JH7-JH1 going from the N-terminus to the C-terminus. These proteins contain four functional domains [69]. The N-terminal JH7-JH6 module corresponds to a FERM domain (F for 4.1 protein, E for ezrin, R for radixin and M for moesin); the FERM domain contains ≈ 350 amino acids and targets proteins to the plasma membrane. The JH5-JH3 segment represents an atypical SH2 domain that interacts with protein-glutamate and fails to bind protein-tyrosine phosphate. The JH5-JH3 segment is followed by a JH2 pseudokinase domain and the C-terminal JH1 segment is the functional protein-tyrosine kinase (Fig. 1 C).

The Janus kinase JH2 and JH1 domains contain a small amino-terminal lobe and large carboxyterminal lobe that contains the canonical α-helices and β-strands first described by Knighton et al. for PKA in 1991 [31]. The K581 and E596 of the pseudokinase of the JAK2 JH2 domain fail to make contact and this corresponds to the inactive "αC_{out}" conformation (Fig. 2D) [39]. The following four amino acids, which are part of a K/E/D/D core, characterize the mechanistic properties of the JAK3 JH1 protein-tyrosine kinase domain. An invariant β3-strand lysine (K855, the *K* of *K*/E/D/D) forms a salt bridge with the αC-glutamate (E871, the *E* of K/*E*/D/D) and also the α- and β-phosphate groups of ATP/ADP (not shown). The catalytic loop consists of HRDLAARN in JAK1, JAK3 and TYK2 and HRDLATRN occurs in JAK2. The JAK3 JH2 pseudokinase domain contains ^{645}HGNVSARK^{652}. The catalytic aspartate in JAK3 (D949), which is the first D of K/E/*D*/D, serves as a base that accepts a proton from the tyrosyl–OH moiety. This residue in the JAK pseudokinase domains is an asparagine, which cannot abstract a proton from the phenolic hydroxyl moiety and contributes to the catalytic latency of the pseudokinase domains. Several important human JAK3 JH1 residues are listed in Table 2 and spine and shell residues are provided in Table 3.

JAK1/3 signaling contributes to the development of inflammatory diseases while JAK1/2 action contributes to the pathogenesis of myeloproliferative neoplasms as well as lymphomas and leukemias. JAK3 participates in the pathogenesis of alopecia areata, an inflammatory disorder [15]. The JAK-STAT pathway conveys extracellular signals from a variety of growth factors, chemokines, cytokines, and hormones to the nucleus and is responsible for the expression of hundreds of protein-encoding genes [70]. Numerous steps are required for the conversion of an extracellular signal into a transcriptional response [71]. First, ligand binding produces conformational changes in the cytokine receptors that lead to protein-tyrosine kinase activation produced by the phosphorylation of two tyrosine residues within the activation segment

of the JH1 domains as mediated by a partner Janus kinase JH1 enzyme. Next, the JH1 protein kinase domains catalyze the phosphorylation of cytokine receptor tyrosine residues that attract the SH2 domain of STATs. The activated JH1 protein kinase domain then catalyzes the phosphorylation of the STAT proteins. These phosphorylated STATS then dimerize and are translocated into the nucleus where they regulate the transcription of target genes.

3. Orally effective targeted covalent inhibitors (TCIs) of protein kinases

3.1. Selected diseases related to the ErbB family of protein kinases

3.1.1. Classification and treatment of lung cancers

EGFR/ErbB1 mutations play an essential role in the pathogenesis of many lung cancers. For example, Herbst et al. found that *ErbB1* protein kinase-domain mutations occur in about 10 % of NSCLC patients in the United States and 30–50 % in Asian patients [72]. These authors reported that the most common mutations include (i) a deletion of five exon-19 residues (^{746}ELREA^{750}) that correspond to a location proximal to the αC-helix and (ii) an exon-21 arginine for leucine substitution (L858R) that is located within the activation segment. Although dozens of *ERBB1* mutations have been discovered in NSCLC, these two mutations account for more than 90 % of the activating *EGFR* mutations found in these malignancies.

Activating mutations of oncokinases are commonly found in or near important regulatory regions such as the glycine-rich loop, the αC-helix, or the activation segment. A frequent process leading to the oncogenic activation of the EGFR entails the destabilization of the dormant enzyme. Yun et al. found that this mechanism responsible for the activation of the L858R EGFR mutant [73]. R858 follows ^{855}DFG^{857} at the beginning of the activation segment. The substitution of the hydrophobic leucine side chain with the larger positively charged arginine side chain precludes the latter's occurrence within the proximal activation segment inhibitory αAL loop while an arginine is easily accommodated in the open configuration of the active EGFR protein kinase domain. Consequently, destabilization of the inactive structure of EGFR leads to enzyme activation and neoplastic transformation.

Several orally bioavailable FDA-approved protein-tyrosine kinase inhibitors target mutant *EGFR* and offer lasting disease control [74]. Treatment choices include: (i) first-generation erlotinib and gefitinib, (ii) second-generation afatinib and dacomitinib, and (iii) third-generation mobocertinib, lazertinib, and osimertinib [74]. Of these antagonists, osimertinib offers longer progression-free and overall survival, along with better intracranial activity. For patients relapsing on first-line nonosimertinib options, circulating tumor DNA of the progressive tumor should be tested for the *EGFR*^{T790M} mutation and, if positive, treated with (i) osimertinib, (ii) erlotinib/bevacizumab combination therapy, (iii) or gefitinib and chemotherapy. See Refs. [75,76] for a summary of lung cancer treatment protocols.

3.1.2. Classification and treatment of breast cancers

Breast cancer is the foremost cause of death from malignancies primarily (breast) or exclusively (uterine cervix, uterine corpus, and ovary) affecting females in the United States and worldwide [77,78]. Breast cancers are classified into three groups, which are not mutually exclusive, for treatment strategies: these include (i) overexpression of the *ERBB2/HER2/NEU* gene, (ii) hormone receptor-positive cancers, and (iii) triple-negative breast cancers. Triple-negative breast cancers refer to those (i) lacking progesterone receptors, (ii) lacking estrogen receptors, and (iii) without *ERBB2/HER2* overexpression or amplification. Wittliff found that *ERBB2/HER2* overexpression occurs in about 20 % of breast cancers while 10–20 % of breast cancers are triple-negative [79]. *ERBB2/HER2* overexpression was associated with poor outcomes prior to the initiation of ErbB2/HER2 targeted therapies. He also reported that receptors for estrogen, progesterone, or both occur in about 80 % of all breast cancers. Furthermore, he reported that about 56 % of breast cancers contain both the estrogen and progesterone receptors while 14 % contain only the estrogen receptor and 9 % contain only the progesterone receptor while 21 % of breast cancers lack both receptors [79].

Surgery is the standard of care for localized breast cancer and is also used for the management of many advanced breast cancers [80]. Other treatment modalities include cytotoxic chemotherapy, radiotherapy, targeted ErbB2/HER2 therapy, immunotherapy, and adjuvant hormonal therapy (with tamoxifen or an aromatase inhibitor) for hormone receptor-positive tumors [80,81]. Immunotherapy and endocrine-based therapy are not as effective in the management of HER2-positive breast cancer as desired and chemotherapy is accompanied by considerable toxicity. Numerous cytotoxic agents are used in the treatment of metastatic breast cancers, especially those cancers that are hormone receptor-negative or triple negative [82]. These cytotoxic agents include cyclophosphamide, doxorubicin, and taxanes. Cyclophosphamide is an alkylating agent that forms both intra and interstrand DNA cross links that disrupt DNA base pairing and structure, replication, and transcription. Doxorubicin is an anthracycline derivative that intercalates with DNA, inhibits topoisomerase II activity, and creates oxygen-dependent single and double stranded DNA breaks. Paclitaxel and docetaxel are antimitotic taxanes that bind to and enhance microtubule polymerization and obstruct their function. In addition to the overexpression of wild type *ERBB2* in breast cancers, Bose et al. reported that approximately 1.5 % of breast cancer patients possess an *ERBB2* mutation [83], which amounts to a few thousand new cases per year in the United States.

About one-fifth of advanced breast carcinomas are HER2-positive [79]. One standard first-line treatment for this disease includes the combination of trastuzumab, pertuzumab, and a taxane [81]. The former monoclonal antibody is directed against the extracellular domain of ErbB2/HER2 and promotes HER2 internalization and down-regulation and stimulates immune cells to kill the HER2-expressing cells. Pertuzumab targets ErbB2/HER2 and precludes its dimerization with other ErbB family members. A standard second-line treatment consists of ado-trastuzumab emtansine; this antibody-drug conjugate delivers the emtansine microtubule inhibitor to ErbB2/HER-positive cells. One follow-up treatment includes the trastuzumab deruxtecan antibody-drug conjugate as a monotherapy following two previous treatments. Deruxtecan damages DNA and causes apoptosis. Another third-line treatment consists of tucatinib, a noncovalent HER2 protein-kinase blocker, in combination with trastuzumab and cytotoxic capecitabine. Additionally, the HER2-TCI neratinib in combination with capecitabine is another third-line treatment option [80,81].

3.2. Diseases related to Bruton tyrosine kinase over activity

Mantle cell lymphomas are B cell disorders that constitute about 6 % of non-Hodgkin lymphomas and patients usually present with palpable lymphadenopathy at a median age of about 65 years [84]. They are more common in men than women with a ratio 4/1. More than two-thirds of patients are at stage IV at the time of diagnosis. Prior to the advent of ibrutinib therapy, the historical median overall survival in patients with newly diagnosed disease was three to four years. Wang et al. reported that ibrutinib produced an elevation of lymphoma cells in the peripheral blood following 10 days of treatment followed by a decrease to baseline values after 28 days of treatment [85]. This transient increase in cells was caused by their liberation from affected lymphatic tissues. The authors suggested that ibrutinib monotherapy was more effective and less stressful than previous standard therapies. Based upon these clinical findings, the FDA approved ibrutinib for the management of mantle cell lymphomas in 2013 [86].

Chronic lymphocytic leukemia (CLL) is a clonal B cell disorder that is the most common type of leukemia in the Western hemisphere; it is

responsible for about 40 % of all adult leukemias [87]. It accounts for about 15,000 new cases per year in the United States corresponding to an incidence rate of 4.5 per 100,000 people. The median age at the time of diagnosis is about 70 years of age. Its diagnosis is oftentimes incidental resulting from routine blood counts. In symptomatic patients, the presenting features can include fever, fatigue, and infections. Clinical studies demonstrated the effectiveness of ibrutinib in the management of small cell lymphomas and chronic lymphocytic leukemias leading to the FDA approval for the treatment of these maladies [88].

Waldenström macroglobulinemia is a B cell disorder linked with the production of clonal immunoglobulin M secreting lymphoplasmacytic cells [89]. The incidence rate is about 0.38 per 100,000 people in the United States, which corresponds to about 1300 cases per year. The median age at the time of diagnosis is about 70 years of age and the ratio of men to women is about 1.5/1. The signs and symptoms of this disease are variable and patients can present with fatigue, headaches, fever, chills, recurrent sinus and bronchial infections, and gastrointestinal distress. Hepatosplenomegaly and lymphadenopathy may also be found. Increased IgM levels (>7 g/dL), which are more than 25 times greater than normal, may occur. These high IgM levels raise serum viscosity, which may produce transient episodes of blurry vision, headaches, and mental confusion. Laboratory findings demonstrate that BTK is constitutively activated in Waldenström macroglobulinemia cells and positive clinical trials led to the FDA approval of ibrutinib for the treatment of this illness. See Ref. [88] for a summary of the clinical efficacy of acalabrutinib, ibrutinib, and zanubrutinib in the treatment of B-cell lymphomas and see Refs. [90,91] for a synopsis of the treatment of Waldenström macroglobulinemia with these TCIs.

3.3. FGFR gene rearrangements and cholangiocarcinoma

Cholangiocarcinoma is an uncommon malignancy that arises from epithelial cells of the extrahepatic and intrahepatic bile ducts. About 8000 to 10,000 people receive the diagnosis of this cancer each year in the United States [92]. About two-thirds of these tumors are intrahepatic and originate in the biliary tract within the liver and are considered distinct from tumors that arise extrahepatically. Laboratory studies indicate that various molecular tumor drivers occur in the intrahepatic subtype. Cholangiocarcinomas have often metastasized at the time of diagnosis with a five-year survival under 10 %. The previous standard-of-care for patients with unresectable or metastatic disease was combination therapy with gemcitabine and cisplatin. In people with advanced disease and disease progression after prior treatment, the median overall survival was about six months. FGFR2 fusions occur in 10-20 % of cholangiocarcinoma patients with most (87 %) of these FGFR2 fusion-positive cases being intrahepatic. Patients with FGFR2 fusions appear to survive longer than those without fusion proteins.

Futibatinib is an inhibitor of the FGFR family, which make up a group of receptor tyrosine kinases that play key roles in cell growth, proliferation, differentiation, and survival [93]. FGFRs were investigated as a therapeutic target because FGFR genomic aberrations and deregulated FGFR signaling pathways were seen in various cancers including cholangiocarcinoma and neoplasms of the urinary tract. Futibatinib is a selective irreversible inhibitor of FGFR 1–4 with IC_{50} values of less than 4 nM. Of 296 protein kinases examined, it had slight activity against MAPK12 and the insulin receptor. It forms a covalent bond with Cys491 in the ATP-binding pocket glycine-rich loop. After its binding, futibatinib blocks FGFR2 autophosphorylation and the phosphorylation of FRS2; FRS2 is an adapter protein that links the activation of FGFRs to downstream intracellular signaling pathways. The main downstream signaling modules of the FGFRs include the (i) PI3K/Akt/mTOR pathway and (ii) the RAS-dependent Raf-MEK-Erk (MAP kinase) pathway. mTOR and Erk mediate the phosphorylation of dozens of cytosolic proteins. Moreover, Erk is translocated into the cell nucleus and catalyzes the phosphorylation and activation of many transcription factors. Futibatinib reduces cell viability in cancer cell lines with FGFR dysregulation including FGFR amplifications, fusions, rearrangements, and mutations.

3.4. JAK3 and alopecia areata

Alopecia areata is an autoimmune disorder that leads to hair loss in the scalp and other regions of the body [94–98]. The ratio of men to women with this disease is 1.7/1.0 and the median age of patients undergoing treatment is 38 years. The JAK-STAT pathway, which controls the levels of various inflammatory mediators, is associated with the pathophysiology of this malady. This disorder, which is challenging to manage, is characterized by recurring periods of hair loss and regrowth [96]. It can be aggravated by anxiety and stress with an adverse effect on the quality of life. People with alopecia areata exhibit scalp hair loss in patches, while patients with more severe disease display complete scalp hair loss (alopecia totalis) or entire body hair loss (alopecia universalis) [99]. As noted above, the JAK family kinases activate STATs. The JAK/STAT pathway increases the production of interferon-γ and interleukin-15 (IL-15), which activate $CD8^+$ T cells. These cells in turn target hair follicle cells and this process participates in the pathogenesis of alopecia areata [96]. The ritlecitinib blockade of JAK3 expressed in hematopoietic cells blunts the immune attack of the hair follicles and decreases the inflammatory response.

Topical corticosteroids were the primary treatments of mild disease, while corticosteroids and the antimetabolites azathioprine or methotrexate were recommended for people with severe disease [97]. These treatments are of low efficacy and better treatment modalities were needed, prompting the development of JAK inhibitors such as the FDA-approved ritlecitinib and deuruxolitinib. Meta analysis of the efficacy of these two agents reveals that their clinical effectiveness is about the same. Other JAK inhibitors are in clinical trials for the management of alopecia areata include baricitinib, ruxolitinib, and tofacitinib (www.clinicaltrials.gov); these three medicines are FDA-approved for the management of other inflammatory diseases [16].

4. Protein kinase-inhibitor classification

Based upon the findings of other investigators [100–103], we divided low molecular weight protein kinase inhibitors into six main groups including reversible (Groups I—V) and irreversible agents (Table 4). We incorporated the results of Liao [104], van Linden et al. [105], and Kanev et al. [106] in depicting and describing drug-binding pockets. A summary describing the location of various pockets and subpockets is provided in Table 5. These authors divided the region between the protein kinase amino-terminal and carboxyterminal lobes into a front pocket or cleft, a gate area, and a back cleft. The back pocket or hydrophobic pocket II (HPII) includes the gate area and back cleft. The front cleft includes the glycine-rich P-loop, the adenine-binding

Table 4
Classification of small molecule protein kinase inhibitors[a].

Inhibitor type	Properties
I	Binds in and around the ATP-binding pocket of an active enzyme
I½ A/B	Binds in and around the ATP-binding pocket of an inactive DFG-D_{in} enzyme
I½ A	Extends into the back cleft
I½ B	Does not extend into the back cleft
II A/B	Bind in and around the ATP-binding site of an inactive DFG-D_{out} enzyme
II A	Extends into the back cleft
II B	Does not extend into the back cleft
III	Allosteric inhibitor bound near to the ATP-binding site
IV	Allosteric inhibitor bound far from the ATP-binding site
V	Bivalent inhibitor spanning two kinase domain regions
VI	Covalent inhibitor

[a] Adapted from Ref. [114].

Table 5
Location of selected catalytic cleft residues[a].

Description	Location	KLIFS residue no.
GxGxΦG	Front cleft	4–9
β2-strand V (CS7)	Front cleft	11
β3-strand A (CS8)	Front cleft	15
β3-strand AxK-K	Front cleft	17
Catalytic loop: HRD(x)$_4$N	Front cleft	68–75
HRD with DFG-D$_{in}$	Front cleft	68–70
HRD(x)$_4$N-N	Front cleft	75
β7-strand CS6	Front cleft	77
αC-β4 back loop residue	Gate area	36
Gatekeeper	Gate area	45
Hinge	Gate area	46–48
Linker	Gate area	49–52
x of xDFG	Gate area	80
DFG	Gate area	81–83
αC-helix E	Back cleft	24
RS3	Back cleft	28

[a] klifs.net

pocket, the hinge, and the catalytic loop (HRD(x)$_4$N). The gate area includes the linker segment connecting the hinge to the large lobe αD-helix and DFG of the activation segment. The back-cleft includes the αC-helix glutamate and RS3. The components that occur in the front cleft, gate area, and back cleft are depicted in Fig. 3 [106].

Van Linden and Kanev et al. formulated a general summary describing ligand and drug interactions with more than 5200 human and mouse protein kinase domains [105,106]. Their KLIFS (kinase–ligand interaction fingerprint and structure) handbook contains a listing of 85 ligand interacting residues found in both the small and large lobes; this directory expedites a comparison of drugs and ligands and aids in the detection of unique and common interactions. Moreover, these authors devised a standard amino acid residue numbering system that expedites the comparison of various protein kinases. Table 3 correlates the KLIFS database nomenclature and the R-spine, shell, and C-spine amino acid residue numbering system and Fig. 4 illustrates the location of the KLIFS residues within the protein kinase domain. Furthermore, these researchers established an effective noncommercial and searchable web site that describe the interaction of ligands and drugs with protein kinases (klifs.net).

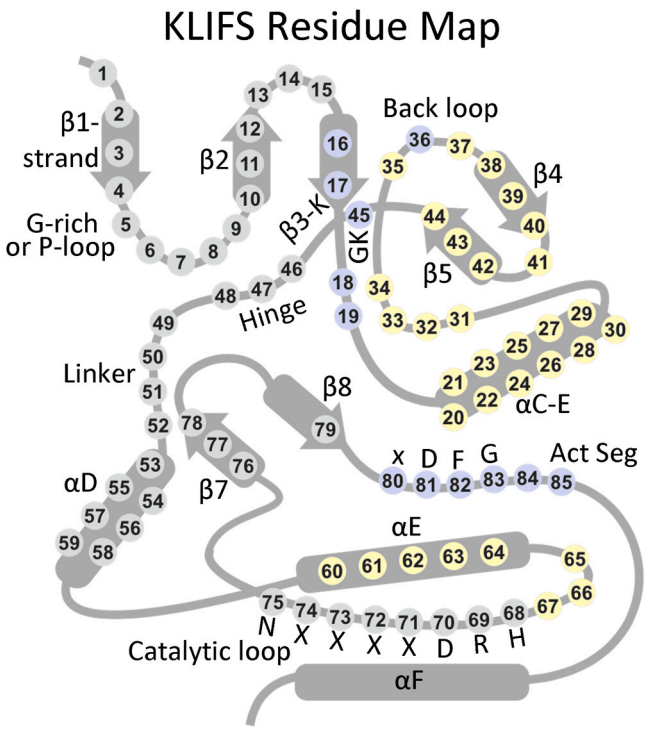

Fig. 4. The location of the KLIFS residues within a generic protein kinase domain. Act Seg, Activation segment. Residues in gray circles are found in the front cleft; blue circles, gate area; yellow circles, back cleft. The figure was kindly provided by Prof. AJ Kooistra.

Moreover, Carles et al. created an extensive catalog of protein kinase inhibitors that have been approved by regulatory agencies or that are in clinical trials [4]. They created a noncommercial and searchable web site that is regularly updated and contains the structure of inhibitors, their physical properties, protein kinase targets, therapeutic indications,

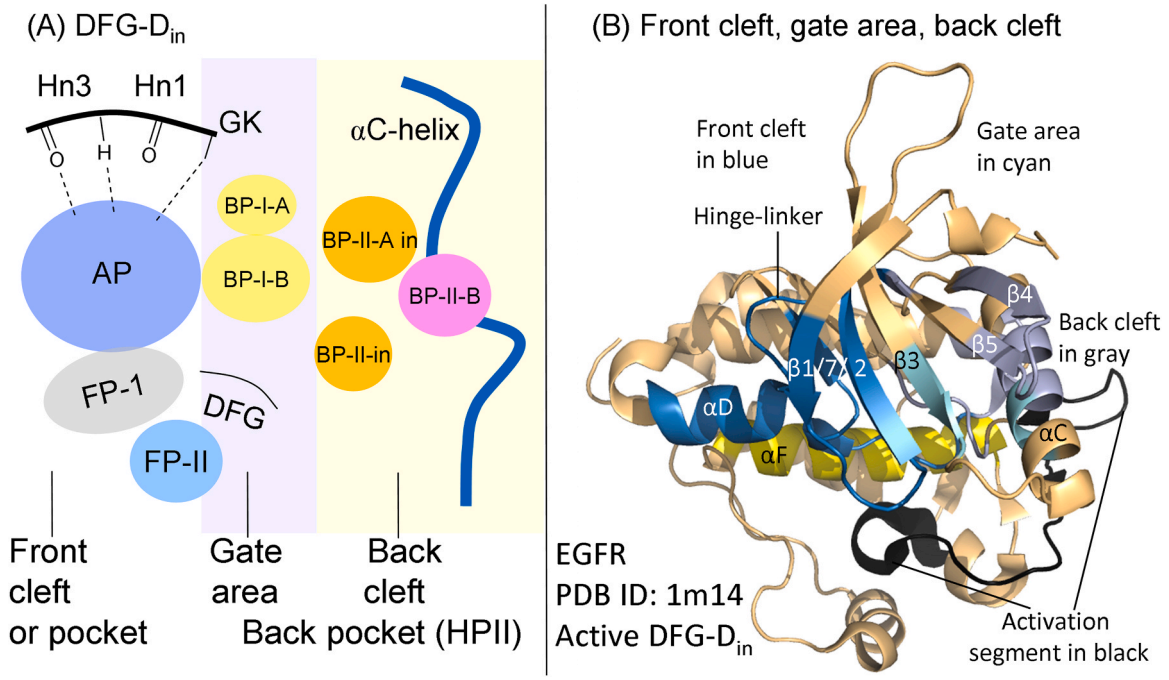

Fig. 3. (A) Location of the protein kinase domain drug-binding pockets. Adapted from Liao [104], van Linden et al. [105], and Kanev et al. [106]. (B) Location of the protein kinase front cleft, gate area, and back cleft. AP, adenine pocket; BP, back pocket; FP, front pocket; Hn, hinge; HPII, hydrophobic pocket II; GK, gatekeeper.

year of first approval, and trade name (http://www.icoa.fr/pkidb/). The Blue Ridge Institute for Medical Research supports a web site that identifies FDA-approved protein kinase inhibitors and provides their (i) structures, (ii) number of hydrogen bond donors/acceptors, (iii) log of the distribution coefficient, (iv) number of rotatable bonds and rings, (v) year of initial FDA approval, (vi) protein kinase targets, and (vii) clinical indications. The site also provides a link to current FDA labels. The address of this regularly updated web site is www.brimr.org/PKI/PKIs.htm.

The eleven medicines reviewed in this article have a shared mechanism of action; the chemistry involves the combination of a protein cysteine thiolate anion (protein—S:¯) with an acrylamide or an acrylamide-like derivative [107]. These reactions are generally called Michael additions and the chemistry involves the formation of a covalent bond between sulfur and carbon and the final product is a thioether (Fig. 5A). Such Michael additions are irreversible. This process involves two discrete steps; the first phase involves the reversible association of the drug with its target enzyme so that a weakly electrophilic warhead or reaction moiety binds near a properly positioned nucleophilic cysteine. The dissociation constant for this part of the process is given by the K_i (Fig. 5B). In the second phase, a reaction between the warhead and the target enzyme cysteine occurs to form a covalently modified and inactive kinase and the rate constant for this reaction is given by k_{inact}. For this chemistry to succeed, the warhead must be appropriately juxtaposed to the cysteinyl thiolate so that the covalent link can be made. The overall velocity of covalent bond formation is given by the second-order rate constant k_{inact}/K_i with units of moles per second (M/s) [9].

5. Structures of drug-enzyme complexes

5.1. EGFR-drug complexes

Afatinib is a 3-chloro-4-fluoroanilino-quinazoline derivative (Fig. 6A) that is FDA-approved for the first-line treatment of people with NSCLC harboring *EGFR*-mutations or as a second-line treatment for individuals with squamous cell NSCLC progressing after platinum-based chemotherapy [108–111]. Afatinib inhibits EGFR/ErbB1 irreversibly *in vitro* with an IC_{50} value of 0.5 nM for wildtype EGFR, 0.4 nM for the *EGFR* L858R mutant, 10 nM for the *EGFR* L858R/T790M double mutant, 14 nM for ErbB2/HER2, and 1 nM for ErbB4 (https://www.ebi.ac.uk/chembl/). Its X-ray crystal structure demonstrates that the quinazoline *N*1 hydrogen bonds with the EGFR M793 (the third hinge residue) N–H group (Fig. 7A) [112]. The drug interacts hydrophobically with four spine residues (RS3, CS6/7/8), two shell residues (Sh2/3), and the KLIFS-3 β1-strand residue (Table 6). Afatinib interacts hydrophobically with K728 of the β2-strand, AxK-K745 of the β3-strand, E762 and M766 of the αC-helix, and L788 of the β5-strand. Furthermore, the medicine interacts hydrophobically with ^{792}LMPFGC^{797} of the hinge-linker. The medicinal also interacts hydrophobically with D800 of the αD-helix, R841 of the catalytic loop, and T854 (the x of xDFG) within the large lobe. The medicine forms a covalent Michael adduct with C797 in the linker segment proximal to the C-terminal lobe αD-helix. The quinazoline moiety is found in the adenine pocket and the 3-chloro-4-fluoroanilino group is found in the gate area (BP-I-A and BP-I-B).

Modi and Dunbrack described eight different protein kinase configurations and classified them based upon the conformation of the phenylalanine rotamer (plus, minus, trans) and on the Ramachandran regions (A, alpha; B, beta; L, left) of the xDF motif [113]. Their classification divides the DFG-D_{in} configuration into six clusters including BLAminus, which represents an active structure and five inactive conformations. Their $DFG_{intermediate}$ structures are found primarily in the BABtrans configuration and the DFG-D_{out} assemblies are found mainly in the BBAminus conformation. Modi and Dunbrack created a useful noncommercial and searchable web site (http://dunbrack3.fccc.edu/kincore/) that allows one to determine whether a given protein kinase structure corresponds to an active or inactive enzyme. We used this web site to ascertain whether the structures of our drug-enzyme complexes correspond to active (DFG-D_{in}, BLAminus) or inactive (otherwise) enzymes. Although afatinib binds to the active BLAminus conformation of EGFR, it is classified as a type VI inhibitor because it is irreversibly bound to its target enzyme [114]. For a summary of the clinical trials that led to its approval, see Ref. [115].

Dacomitinib, like afatinib, is a 3-chloro-4-fluoroanilino-quinazoline derivative and it forms a covalent adduct with EGFR/ErbB2/ErbB4 (Fig. 6B) [25]. The drug is approved for the first-line management of people with metastatic NSCLC with an *EGFR* exon 19 deletion or the exon 21 L858R substitution mutation [116–120]. Kooijman et al. reported that the IC_{50} value of the drug for EGFR is 0.27 nM and those for ErbB2/4 were an order of magnitude higher [121]. Gajiwala et al. determined the X-ray crystal structure of dacomitinib with EGFR [122]; it shows that the *N*1 nitrogen of the quinazoline group hydrogen bonds with the M793 N–H group (the third hinge residue) of the *EGFR* T790M mutant (Fig. 7B). The drug interacts hydrophobically with four spine residues (RS3, CS6/7/8), two shell residues (Sh2/3), and the KLIF-3 residue in the β1-strand. The medicine also makes hydrophobic contact with the β3-strand I744 and K745, ^{788}LITQLMPFGC^{797} of the hinge-linker segment, D800 of the αD-helix, T854 (the x of xDFG), and DFG-D855. The dacomitinib acrylamide group of the drug forms a covalent Michael adduct with C797 within the kinase hinge-linker. The medicine is found in the front pocket, gate area, and sub-pocket BP-I-B (klifs.net). The drug binds to a BLAminus active enzyme with DFG-D_{in},

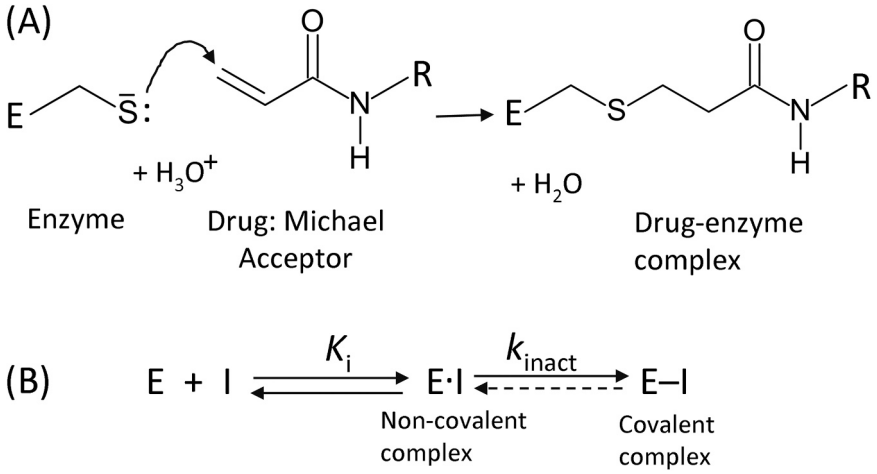

Fig. 5. (A) Michael addition reaction. (B) Two steps in the Michael addition.

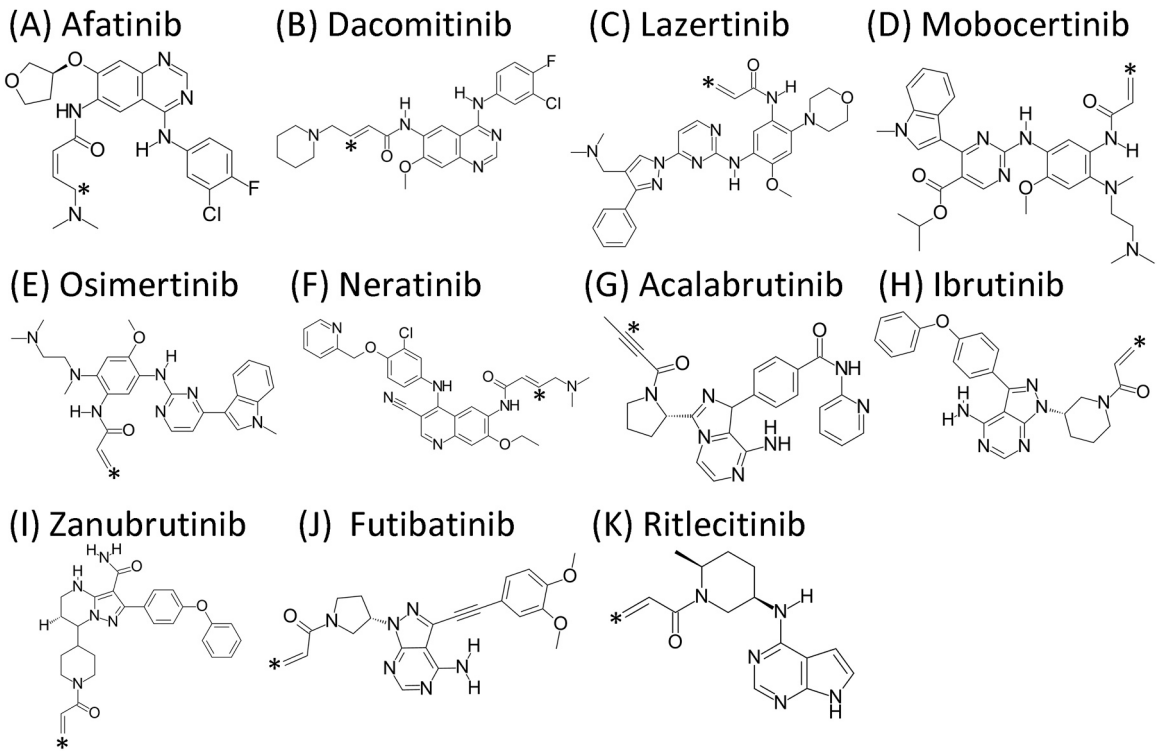

Fig. 6. Structures of selected targeted covalent inhibitors. The asterisks indicate the site where the covalent modification with the protein-cysteine thiolate anion occurs.

αC_{in}, and an open activation segment [113]. Because it is bound irreversibly to its target, dacomitinib is grouped with type VI inhibitors [114]. One mechanism of dacomitinib resistance results from an *EGFR* C797S mutation [123], the serine of which is unable to form a covalent adduct with the drug. For a summary of the clinical trials that led to the FDA approval of dacomitinib, see Refs. [119,124].

Lazertinib is a pyrazole-pyrimidine derivative (Fig. 6C) and TCI that is FDA-approved for the first-line treatment of adult patients with locally advanced or metastatic non-small cell lung cancer (NSCLC) with an epidermal growth factor receptor (EGFR) exon 19 deletion or an exon 21 L858R substitution mutation in combination with amivantamab [16]. Amivantamab is a monoclonal antibody that binds to both MET (the hepatocyte growth factor receptor protein-tyrosine kinase) and EGFR and blocks the binding of their activating ligands and stimulates receptor internalization and degradation. Heppner et al. determined the X-ray crystal structure of the EGFR-lazertinib complex [124] and found that the *N*1 pyrimidine nitrogen forms a hydrogen bond with the N–H group of M793 – the third hinge residue – and the attached amino moiety forms a hydrogen bond with the carbonyl oxygen of M793 (Fig. 7 C). Lazertinib interacts hydrophobically with four spine residues (RS3, CS6/7/8), and the Klifs-3 residue. The drug also makes hydrophobic contact with the β1-strand L718 before the G-rich loop, the conserved β3-strand AxK-K745, ^{791}QLMP^{794}, G796, and C797 of the hinge-linker segment, D800 of the αD-helix, R841 and N842 of the catalytic loop, T845 (the x residue of xDFG), and DFG-D855. Lazertinib is found in the front pocket of a protein kinase in an active configuration with DFG-D_{in}, αC_{in}, and an open activation segment with an overall active BLAminus conformation [113]; because of the irreversible nature of the covalent modification of its target enzyme, it is classified as a type VI inhibitor [114]. One benefit of lazertinib is that it is more effective vs. the *EGFR T790M* mutant (K_i = 2.7 nM) than the wildtype enzyme (K_i = 34.6 nM). This characteristic decreases the potential for drug-induced side effects. See Refs. [125,126] for a summary of the investigations that led to the approval of this combination therapy for *EGFR* mutation-positive NSCLC.

Mobocertinib is an anilino-pyrimidine derivative (Fig. 6D) that antagonizes EGFR and is FDA-approved for the treatment of adult patients with locally advanced or metastatic NSCLC with EGFR exon 20 insertion mutations, as detected by an FDA-approved test, whose disease has progressed on or after platinum-based chemotherapy (Supplementary material). Mobocertinib potently inhibited the growth of Ba/F3 cells with the activating *EGFR* deletion mutant (IC_{50} value of 2.7 nM), the L858R substitution mutant (3.3 nM), and the *EGFR* L858R/T790M double mutant (21.3 nM) [127]. Significantly, mobocertinib blocked these *EGFR* mutants with selectivity over wildtype EGFR (IC_{50} = 34.5 nM) that diminishes the potential for unwanted side effects [127]. The X-ray crystal structure [127] shows that the anilino N–H hydrogen bonds with the carbonyl group of M793 and the N–H group of M793 hydrogen bonds with one of the pyrimidine nitrogen atoms (Fig. 7D). The drug makes hydrophobic contact with three spine residues (CS7/8/9), two shell residues (Sh2/3), and the Klifs-3 residue (Table 6). The drug also interacts hydrophobically with G719 and F723 of the glycine-rich loop, I744 and K745 of the β3-strand, L788 of the β5-strand, T790 (the gatekeeper residue), and residues L792, M793, P794, G796, C797 of the hinge-linker segment. The drug is found in the front pocket, gate area, and BP-I-A/B. The enzyme is in the active BLAminus conformation with an open activation segment, αC_{in}, and DFG-D_{in} [113]. Owing to the irreversible nature of the inhibition, mobocertinib is classified as a type VI inhibitor [114]. See Ref. [128] for a summary of the clinical trials that led to the FDA approval of this medicine.

Osimertinib is an indole-pyrimidine derivative (Fig. 6E) that is FDA-approved for the initial or first-line treatment of people with metastatic NSCLC bearing an *EGFR* exon-19 deletion or an exon 21 L858R mutation [129]. The agent is also approved for the second-line treatment of patients with metastatic *EGFR* T790M-positive NSCLC that has progressed on or after EGFR small molecule inhibitor therapy. This was the first targeted medicinal that was approved for patients with the gatekeeper *EGFR* T790M drug-resistant variant [130]. Osimertinib is more effective than either erlotinib or gefitinib in treating people with *EGFR*-positive NSCLC brain metastases [111]. Osimertinib exhibits an IC_{50} of 12.9 nM

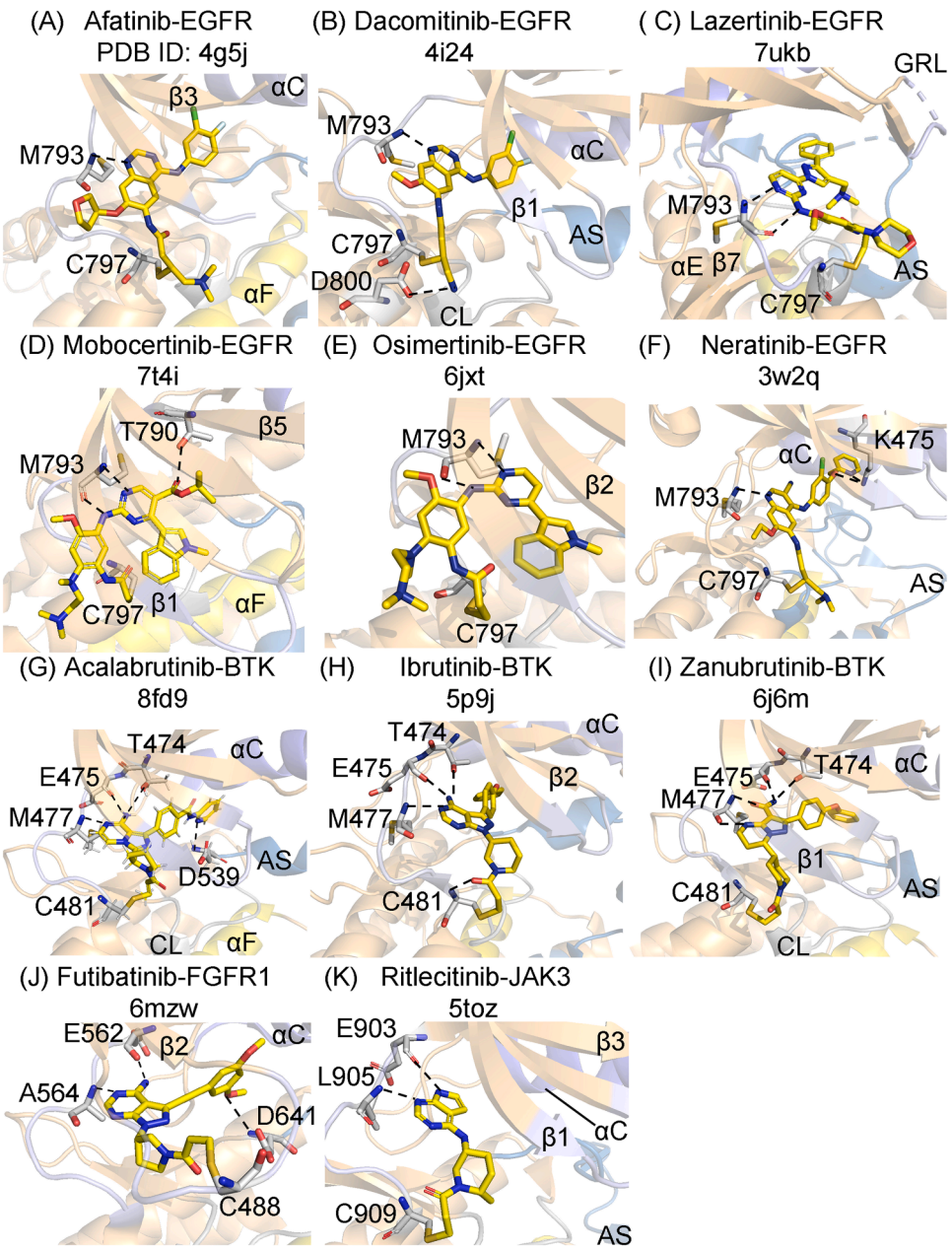

Fig. 7. Structures of selected drug-enzyme complexes. The PDB ID is listed. The carbon atoms of the drugs are colored yellow. The dashes represent polar bonds. AS, activation segment; CL, catalytic loop.

against *EGFR* cell lines carrying exon 19 deletions (https://www.ebi.ac.uk/chembl/). It also inhibits cell lines with the *EGFR* L858R/T790M double mutation with an IC_{50} of 11.4 nM. In contrast, osimertinib has a much higher IC_{50} value (494 nM) against wildtype EGFR that decreases the potential for adverse events owing to the blockade of wildtype EGFR. The X-ray crystal structure reveals that a pyrimidine nitrogen forms a hydrogen bond with the N–H group of the third hinge residue (M793) and a drug amino N–H group forms a hydrogen bond with the carbonyl group of this residue (Fig. 7E) [130]. The drug makes hydrophobic contact with three spine residues (CS6/7/8) and with the KLIFS-3 residue. It also makes hydrophobic contact with K745 of the β3-strand, ^{792}LMP^{794} of the hinge, G796 and C797 of the hinge-linker, and DFG-D855. The acrylamide group forms a covalent Michael adduct with C797. Osimertinib binds chiefly within the front pocket of a protein in a dormant conformation (DFG-D_{in}, αC_{out}, and a closed activation segment). According to the Modi and Dunbrack classification, the protein assumes the inactive BLBtrans conformation [113]. Osimertinib is classified as a type VI inhibitor because it forms a covalent bond with its target protein kinase (Table 4) [114]. Drug resistance mutations occur in almost all cancer patients treated with protein kinase inhibitors [1] and osimertinib is no exception. One mechanism of osimertinib resistance results from a C797S mutation [122].

Neratinib is an anilino-quinazoline derivative (Fig. 6F) that irreversibly inhibits ErbB2 and is FDA-approved for the extended adjuvant management of adult patients with early stage ErbB2-overexpressed/amplified breast cancers following adjuvant trastuzumab-based treatment [131–134]. The drug is a potent inhibitor of EGFR (IC_{50} value of 1.1 nM), the *EGFR* T790M mutant (1.5 nM), the *EGFR* L747-T751 deletion mutant (1.0 nM), the *EGFR* G719S substitution mutant (0.91 nM), HER2 (6.0 nM), and ErbB4 (2.4 nM) (https://www.ebi.ac.uk/chembl/). Although there are no X-ray crystal structures of neratinib bound to ErbB2, its presumed primary target in patients with breast cancer, we have the structure of the antagonist bound to the *EGFR* gatekeeper (T790M) mutant (PDB ID: 2jiv) and the *EGFR* L858R/T790M

Table 6
Drug-enzyme hydrophobic (Φ) interactions based upon their common KLIFS residue numbers[a,b].

	PDB ID	RS1	RS2	RS3	RS4	Sh1	Sh2	Sh3	CS5	CS6	CS7	CS8	KLIFS−3[c]	C[d]/D[e]	KLIFS pockets
KLIFS no. →		68	82	28	38	36	45	43	76	77	11	15	3		
Drug-enzyme ↓															
EGFR complexes															
Afatinib-EGFR	4g5j			Φ			Φ	Φ		Φ	Φ	Φ	Φ	in/in	F, G, BP-I-A/B
Dacomitinib-EGFR	4i23			Φ			Φ	Φ		Φ	Φ	Φ	Φ	in/in	F, G, BP-I-A/B
Lazertinib-EGFR	7ukv			Φ						Φ	Φ	Φ	Φ	in/in	F
Mobocertinib-EGFR	4t4i						Φ	Φ		Φ	Φ	Φ	Φ	in/in	F, G, BP-I-A/B
Osimertinib-EGFR	6jxt									Φ	Φ	Φ	Φ	out/in	F
ErbB2/HER2-like complex															
Neratinib-EGFR	2jiv			Φ	Φ		Φ	Φ		Φ	Φ	Φ	Φ	out/in	F, G, B, BP-I-A/B
BTK complexes															
Acalabrutinib-BTK	8fd9		Φ	Φ	Φ		Φ	Φ	Φ	Φ	Φ	Φ	Φ	out/in	F, G, BP-I-B
Ibrutinib-BTK	5p9j		Φ	Φ		Φ	Φ	Φ		Φ	Φ	Φ	Φ	out/in	F, G, B, BP-I-B
Zanubrutinib-BTK	6j6m		Φ	Φ		Φ	Φ	Φ		Φ	Φ	Φ	Φ	out/in	F, G, B, BP-I-B
FGFR1 complex															
Futibatinib-FGFR1	6mzw		Φ	Φ		Φ	Φ	Φ		Φ	Φ	Φ	Φ	in/in	F, G, B, BP-I-A/B
JAK complex															
Ritlecitinib-JAK3	5toz					Φ	Φ			Φ	Φ	Φ	Φ	in/in	F

[a] klifs.net
[b] Drug-enzyme hydrophobic (Φ) interactions
[c] KLIFS-3, kinase-ligand interaction fingerprint and structure residue
[d] αCin/out
[e] DFG-Din/out

double mutant (PDB ID: 3w2q) [135,136]. The *N*1 of neratinib hydrogen bonds with the N–H group of M793 (the third hinge residue) of the double mutant (Fig. 7F). The medicinal also forms two hydrogen bonds with AxK-K475 of the β3-strand. The drug makes hydrophobic contact with five spine residues (RS3/4 and CS6/7/8), two shell residues (Sh2/3), and the KLIFS-3 residue (Table 6). The drug also interacts hydrophobically with the β3-strand I744 and K745, αC-helix residues I759, E762, and A763, the β4-strand L777, hinge residues ^{791}QLMPFGC^{797}, the αD-helix residue D800, and R841 of the catalytic loop. The drug binds to the front pocket, gate area, back pocket, and BP-I-A/B (Klifs.net). The drug binds to an inactive BLBplus conformation of the enzyme with αC_{out}, DFG-D_{in}, and a disordered activation segment [113]. Neratinib binds irreversibly to its target and is classified as a type VI inhibitor [114]. It is likely that this drug binds to ErbB2, its presumed therapeutic target, in a similar fashion. For a discussion of the clinical trials that led to its approval, see Ref. [137].

To recap this section, the medicines that bind to EGFR form a hydrogen bond with the third hinge residue and they make hydrophobic contact with the β1-strand L718, the β2-strand V726 (CS7), the β3-strand A743 (CS8), L792 (the second hinge residue), and the β7-strand L844 (CS6) on the floor of the adenine pocket (Table 6). The six medications occur in the front pocket and only neratinib extends into the back pocket. With the exception of mobocertinib, the medicines interact hydrophobically with RS3. Afatinib, dacomitinib, mobocertinib, and neratinib occupy the BP-I-A and BP-I-B subpockets in the gate area.

5.2. Bruton tyrosine kinase-drug complexes

Acalbrutinib is a targeted covalent inhibitor and amino-pyrazine derivative (Fig. 6G) that blocks BTK (IC_{50} value of 3 nM) and is FDA-approved for the treatment of mantle cell lymphoma, chronic lymphocytic leukemia, and small lymphocytic lymphoma (Supplementary material). Lin and Andreotti determined the X-ray crystal structure of the drug covalently bound to mouse BTK [138]. The protein kinase domain of the mouse enzyme (residues 401–655) differs by only three residues from that of the human protein and we assume that the mouse enzyme represents an appropriate surrogate for the human protein. The X-ray structure indicates that the amino group attached to the pyrazine moiety forms hydrogen bonds with the side chain of T474 (the gatekeeper) and the carbonyl group of E475 (the first hinge residue). A pyrazine nitrogen hydrogen bonds with the carbonyl group of M477 (the third hinge residue). The pyridine nitrogen of the drug hydrogen bonds with the backbone carbonyl group of DFG-D539 (Fig. 7G). The drug makes hydrophobic contact with six spine residues (RS2/3/4, CS6/7/8), two shell residues (Sh2/3), and the Klifs −3 residue. The drug interacts hydrophobically with ^{409}GTG^{411} of the G-rich loop, R430 of the β3-strand, M449 of the αC-helix, L460 of the β4-strand, I472 of the β5-strand, Y476, M477, G480, C481 of the hinge-linker segment, R525 and N526 of the catalytic loop, S538 (the x of xDFG), DFG-D539, DFG-F540, and M542 of the activation segment. The drug occupies the front pocket, the gate area, and BP-I-B. The enzyme exists in an inactive BLBplus configuration with αC_{out}, DFG-D_{in}, and a closed activation segment [113]. Owing to the covalent nature of the inhibitor, acalabrutinib is classified as a type VI inhibitor [114]. See Refs. [139–141] for synopses on the use and efficacy of acalabrutinib.

Ibrutinib is a pyrazolo[3,4-*d*]pyrimidine derivative (Fig. 6H) that inhibits BTK (IC_{50} value of 0.5 nM) and is FDA-approved for the management of the six disorders that are listed in Table 1 [142]. The X-ray crystal structure [143] shows that the *N*3 pyrimidine form a hydrogen bond with the backbone N–H group of the third hinge residue (M477) and the 4-amino group hydrogen bonds with the –OH group of the threonine gatekeeper residue (T474) and the carbonyl group of the first hinge residue (E475) (Fig. 7H). The drug carbonyl group also forms a hydrogen bond with the C481 residue within the hinge-linker immediate before the αD-helix. The acrylamide group forms a covalent Michael addition product with the same C481. The medicinal makes hydrophobic contact with five spine residues (RS2/3 and CS6/7/8), three shell residues (Sh1/2/3), and the KLIFS-3 residue preceding the glycine-rich loop (Table 6). The agent also makes hydrophobic contact with the first residue of the glycine-rich loop (G409), the β3-strand AxK-K430, the hinge-linker residues Y476, M477, and C481, the αD-helix N484, S538 (the x of xDFG), DFG-D539, DFG-F540, and L542 of the activation segment. The drug occupies the front and back pockets, the intervening gate area, and BP-I-B. Ibrutinib binds to an inactive BLBplus enzyme with αC_{out}, DFG-D_{in}, and a closed activation segment [113]. Ibrutinib is classified as a type VI inhibitor owing to the formation of a covalent bond with its drug target [114]. See Refs. [6,37,85,142] for a summary of the clinical trials that led to the approval of this medicine.

Zanubrutinib is a 4,5,6,7-tetrahydropyrazolo[1,5-*a*]pyrimidine derivative (Fig. 6I) that inhibits BTK (IC_{50} = 1.5 nM) and is FDA-approved for the treatment of mantle cell lymphoma [144,145]. The X-ray crystal structure shows that the N–H group of the pyrimidine forms a hydrogen

bond with the carbonyl group of the third hinge residue (M477) and the carboxamide carbonyl moiety forms a hydrogen bond with the N–H group of this same residue [146]. The carboxamide N–H moiety hydrogen bonds with the carbonyl group of E475 and the –OH group of the gatekeeper T474 (Fig. 7I). The drug makes hydrophobic contact with five spine residues (RS2/3 and CS6/7/8), three shell residues (Sh1/2/3), and the KLIFS-3 residue preceding the glycine-rich loop. The antagonist also makes hydrophobic contact with the β3-strand AxK-K430, the gatekeeper T474, hinge-linker residues Y476, M477, G480, C481, and αD-helix residues L483 and N484, catalytic loop residue R525, S538 (the x of xDFG), DFG-D539, DFG-F540, and L542 of the activation segment. The drug forms a covalent bond with C481 at the end of the hinge-linker segment. Like ibrutinib, zanubrutinib occupies the front and back pockets, the intervening gate area, and BP-I-B. The drug binds to an inactive BLBplus enzyme with αC_{out}, DFG-D_{in}, and a closed activation segment [113]. Zanubrutinib is classified as a type VI inhibitor owing to the formation of a covalent bond with its medicinal target [114]. See Ref. [147] for a summary of the clinical trials that led to the approval of this medicine.

5.3. Futibatinib-FGFR1

Futibatinib is a pyrazolo[3,4-*d*]pyrimidine product (Fig. 6J) that blocks FGFR1/2/3/4 with IC_{50} values of 3.9/1.3/1.6/8.3 nM, respectively; consequently, the drug is classified as a pan-FGFR antagonist [148]. The drug is FDA-approved for the treatment of adult patients with previously treated, unresectable, locally advanced or metastatic intrahepatic cholangiocarcinomas harboring fibroblast growth factor receptor 2 (FGFR2) gene fusions or other rearrangements (Supplementary material). Kalyukina et al. determined the X-ray crystal structure of this medicine covalently attached to C488 within the glycine-rich loop of FGFR1 [148]. The structure shows that the 4-amino group of the pyrimidine forms a hydrogen bond with the carbonyl group of E562 (the first hinge residue) and *N*3 forms a hydrogen bond with the N–H group of A564 (Fig. 7J). A methoxy oxygen atom forms a hydrogen bond with the backbone N–H group of DFG-D641. Futibatinib interacts hydrophobically with five spine residues (RS2/3 and CS6/7/8), all three shell residues (Sh1/2/3), and the KLIFS-3 residue (Table 6). The compound also makes hydrophobic contact with F489 of the glycine-rich loop, the β2-strand V492, the β3-strand AxK-K514, the αC-helix E531 and M535, Y563 of the hinge, A640 (the x of xDFG), and DFG-D641. We assume that its interaction with FGFR2 is similar. The compound occupies the front cleft, gate area, back cleft and BP-I-A/B. The drug-enzyme complex assumes an inactive BLAplus conformation with αC_{in}, DFG-D_{in}, and a disordered activation segment [113]. As an irreversible kinase antagonist, we classify it as a type VI inhibitor [114]. Like the FGFR inhibitor erdafitinib, futibatinib produces hyperphosphatemia, which can lead to soft tissue mineralization and calcification [149]. See Ref. [92] for a summary of the clinical studies that led to the FDA approval of futibatinib.

5.4. Ritlecitinib-JAK3

Ritlecitinib is a pyrrolo[2,3-*d*]pyrimidine derivative (Fig. 6K) that blocks the action of JAK3 (IC_{50} value of 0.4 nM) and is FDA-approved for the treatment of severe alopecia areata in adults and adolescents 12 years and older [150]. The X-ray crystal structure shows that the pyrrole N–H forms a hydrogen bond with the backbone carbonyl oxygen of E903 (the first hinge residue) and a pyrimidine N forms a hydrogen bond with the N–H group of L905 (the third hinge residue) [151]. The drug forms a hydrogen bond and a covalent bond with C909 at the end of the hinge-linker (Fig. 7 K). The drug makes hydrophobic contact with three spine residues (CS6/7/8), two shell residues (Sh1/2), and the Klifs-3 residue (Table 6). Ritlecitinib also interacts hydrophobically with G821 of the glycine-rich loop, M909 (the gatekeeper), and Y904 and L905 of the hinge-linker segment. The drug occupies the front pocket. Modi and Dunbrack classify the enzyme as a member of the active BLAminus conformation with αC_{in}, DFG-D_{in}, and an open activation segment [113]. Owing to the covalent interaction of the drug with its target, we classify ritlecitinib as a type VI inhibitor [114].

6. Epilogue

Targeted covalent inhibitors possess several potential advantages which include high potency, efficacy at low doses (100 mg or less daily), and sustained inhibition that requires protein biosynthesis *de novo* to restore target enzyme action [152]. Moreover, targets for these drugs include enzymes, receptors, and proteins with shallow binding sites not responsive to conventional approaches. The potential to block targets previously considered to be undruggable due to the lack of a small-molecule binding pocket has been applied to the formulation of antagonists of the KRAS protein (Kirsten rat sarcoma viral oncogene homolog, which was discovered by Werner H. Kirsten – an Assistant Professor of Pathology at the University of Chicago – in 1967).

RAS mutations are the most common oncogenic alteration in human cancers [153,154]. These proteins are small 21 kDa GTP-binding proteins that function within intracellular signaling cascades resulting from receptor protein-tyrosine kinase activation. *KRAS* mutations are the most prevalent followed by *NRAS;* mutations of *HRAS* are comparatively rare [155]. More than 80 % of pancreatic cancers and more than 30 % of bile duct, colorectal, and lung carcinomas possess activating mutations of the *KRAS* gene. Exon 2 substitutions are the most common KRAS modification and involve the transformation of glycine-12 to aspartate, alanine, arginine, cysteine, serine, or valine. The *KRAS* G12C mutation occurs in about 35 % of lung and ovarian carcinomas, 20 % of endometrial and cholangial malignancies, and 5 % of colorectal cancers. *KRAS* mutations increase the cellular level of the active GTP-bound state and promote cell growth, proliferation, and survival.

The absence of an appropriate small molecule binding pocket in KRAS makes the fabrication of small molecule antagonists difficult. The *KRAS* G12C mutant protein contains a pocket next to the GTP-binding site the modification of which has the potential to lock the protein into an inactive state with GDP-bound. One strategy to inhibit *KRAS* mutants is to employ a GDP-mimetic inhibitor to covalently lock the protein in an inactive GDP-bound state by targeting the Cys12 –SH group. See Ref. [156] for a review of the development of various KRAS TCIs that have achieved considerable clinical success.

In the protein kinase arena, afatinib, dacomitinib, and lazertinib are effective in the treatment of patients harboring EGFR exon 19 deletions and L858R mutants that are not inhibited by first-generation reversible antagonists including erlotinib, gefitinib, and lapatinib. Osimertinib is the treatment of choice for those patients bearing the *EGFR* T790M mutation. This mutant has a lower K_m value (higher steady-state affinity) for ATP than the wildtype enzyme and this property blunts the inhibitory efficacy of reversible EGFR antagonists [135]. This differential becomes inconsequential following the covalent inhibition of the T790M mutant because ATP cannot bind to the modified enzyme.

TCIs have been fabricated by incorporating an electrophilic warhead into compounds that bind to the desired target with high affinity[157]. Many warheads can react with protein-bearing nucleophiles such as aspartate, cysteine, lysine, or tyrosine. The Michael addition is the most widely used procedure for forming covalent linkages with target proteins. Functional groups that undergo such reactions include acrylamides such as futibatinib, ibrutinib, lazertinib, mobocertinib, osimertinib, ritlecitinib, and zanubrutinib, β-substituted acrylamides including afatinib, dacomitinib, and neratinib, and alkynyl amides such as acalabrutinib (Fig. 6). Jackson et al. reported that substituents at the α- or β-position of the Michael acceptor influence the rate of thioether formation [157]. Electron withdrawing moieties at the α-position increase the rate of addition. Conversely, electron donating fragments including electron-rich alkyl or aryl groups at the α- or β-position decrease the rate of thiol addition in comparison with unsubstituted Michael acceptors.

Besides Michael acceptors, activated acetylenes, epoxides, aziridines, vinyl sulfones, and α-haloketones are warheads that can function as irreversible inhibitors following a reaction with cysteinyl residues [158–161]. On the other hand, aldehydes, carbonitriles, α-ketoamides, ketones, cyanamide, α-cyanoacrylamide, α-ketoheterocycles, and boronic acid derivatives are warheads that function as reversible covalent protein-cysteine inhibitors. Warheads have been developed to form covalent bonds with residues other than cysteine. These include vinyl sulfones and vinyl sulfonamides that react with protein-lysines and cysteines while sulfonimidoyl fluorides, sulfonyl fluorides, and aryl fluorosulfates react with protein-lysines and tyrosines. Sulfonyl fluorides can also modify serine, threonine, and histidine residues. Moreover, *N*-Acyl-*N*-alkyl sulfonamides react with surface-exposed protein-lysines and 2-carbonylarylboronic acids are reversible inhibitors that form covalent adducts with protein-lysines. *N*-methyl isoxazolium derivatives react with protein-aspartates, glutamates, and cysteine while oxaziridine complexes combine with protein-methionines. See Refs. [159,160] for an all-inclusive list showcasing warhead structures, classes, and properties.

One of the possible unwanted side effects of covalent inhibitors is the potential to generate immune-mediated adverse events initiated by the modification of target or off-target proteins [158,159]. Although the drug and its protein target alone may not be immunogenic, the resulting complex can become immunogenic by a process called haptenization where the covalently attached drug is the hapten. On rare occasions, covalent drug–protein products are immunogenic and produce idiosyncratic reactions, often weeks or months after the initiation of therapy [158]. Notwithstanding matters connected to the creation of potentially harmful immunogenic drug-protein covalent complexes, the development of effective covalent-based therapies has led to the identification of medicinal properties that minimize the risk of targeted covalent therapy. These properties include (i) minimizing formation of reactive metabolites from cytochrome P450-mediated oxidations and (ii) promoting high selectivity in target engagement allowing for increased potency [161].

In an analysis of the protein kinase cysteinome, Liu et al. examined targetable residues in and around the ATP-binding site [152]. These authors described six cysteinyl targets including one at the hinge-linker end that occurs (i) in the EGFR family members ErbB1/2/4 (corresponding to EGFR C797), the TEC family including BTK, BMX, TEC, TXK, and ITK, Blk (a Src family member), JAK3, MKKa7, and (ii) within the glycine-rich loop of FGFR, (iii) in the solvent area found in JNKs, (iv) in the roof of the pocket found in the NEK2 and RSK enzymes, (v) in the catalytic loop of PDGFR and Kit, and (vi) immediately preceding the DFG of VEGFR, ERK2, and GSK3β. Cysteines represent advantageous targets because they constitute a small fraction (~2.2 %) of amino acid residues found in proteins [162] (decreasing the possibility of adventitious reactions) and they are not conserved as are the HRD, DFG, or the APE signatures.

Similarly, Zhao and Bourne studied potential cysteinyl targets in the protein kinase kinome [163]. They identified targets in 12 regions in different protein kinases including (i) the glycine-rich loop, (ii) the front pocket, (iii) the gatekeeper, (iv) the gatekeeper + 1, (v) the x residue of xDFG, (vi) DFG + 2, (vii) the roof of the ATP-binding site, (viii) a lysine within the roof, (ix) two residues prior to HRD of the catalytic loop, (x) the activation segment, (xi) the extended front pocket, and (xii) remote cysteines. These investigators reported that 208 protein kinases have a least one cysteine in the drug binding site [164]. Wang et al. expanded the repertoire of the protein kinase cysteinome by using a covalent fragment approach involving 47 protein kinases [165]. Leproult et al. considered the design and strategy of preparing selective protein kinase TCIs [166]. They suggested that the protein kinase target residues should not be conserved in order to maximize the selectivity of the antagonist and limit drug toxicity. Covalent inhibitors have arisen from the ranks of drugs to be avoided to become an emerging paradigm. Much of this success can be ascribed to the clinical effectiveness of ibrutinib [6] as well as the other inhibitors reported in this article. Furthermore, the covalent inhibitor approach has gained acceptance as a valuable component of the medicinal chemist's toolbox and is making a significant impact on the fabrication of enzyme inhibitors and receptor modulators [158].

Declaration of Competing Interest

The author is unaware of any affiliations, memberships, or financial holdings that might be perceived as affecting the objectivity of this review.

Acknowledgments

The colored figures in this paper were evaluated to ensure that their perception was accurately conveyed to colorblind readers [167]. The author thanks Laura M. Roskoski for providing editorial and bibliographic assistance. I also thank Josie Rudnicki and Jasper Martinsek help in preparing the figures and Pasha Brezina and W.S. Sheppard for their help in structural analyses. Dr. Albert J. Kooistra provided the template depicted in Fig. 4.

Appendix A. Supporting information

Supplementary data associated with this article can be found in the online version at doi:10.1016/j.phrs.2025.107805.

Data availability

No data was used for the research described in the article.

References

[1] R. Roskoski Jr., A historical overview of protein kinases and their targeted small molecule inhibitors, Pharm. Res. 100 (2015) 1–23, https://doi.org/10.1016/j.phrs.2015.07.010.
[2] P. Cohen, Protein kinases – the major drug targets of the twenty-first century? Nat. Rev. Drug Discov. 1 (2002) 309–315, https://doi.org/10.1038/nrd773.
[3] G.K. Kanev, C. de Graaf, I.J.P. de Esch, R. Leurs, T. Würdinger, B.A. Westerman, A.J. Kooistra, The landscape of atypical and eukaryotic protein kinases, Trends Pharm. Sci. 40 (2019) 818–832, https://doi.org/10.1016/j.tips.2019.09.002.
[4] F. Carles, S. Bourg, C. Meyer, P. Bonnet, PKIDB: a curated, annotated and updated database of protein kinase inhibitors in clinical trials, pii: E908, Molecules 23 (4) (2018), https://doi.org/10.3390/molecules23040908.
[5] C.C. Ayala-Aguilera, T. Valero, Á. Lorente-Macías, D.J. Baillache, S. Croke, A. Unciti-Broceta, Small molecule kinase inhibitor drugs (1995-2021): medical indication, pharmacology, and synthesis, J. Med Chem. 65 (2022) 1047–1131, https://doi.org/10.1021/acs.jmedchem.1c00963.
[6] S.E. Dalton, O. Di Pietro, E. Hennessy, A medicinal chemistry perspective on FDA-approved small molecule drugs with a covalent mechanism of action, J. Med Chem. 13 (68) (2025) 2307–2313, https://doi.org/10.1021/acs.jmedchem.4c02661.
[7] G. Manning, D.B. Whyte, R. Martinez, T. Hunter, S. Sudarsanam, The protein kinase complement of the human genome, Science 298 (2002) 1912–1934, https://doi.org/10.1126/science.1075762.
[8] F.M. Ferguson, N.S. Gray, Kinase inhibitors: the road ahead, Nat. Rev. Drug Discov. 17 (2018) 353–377, https://doi.org/10.1038/nrd.2018.21.
[9] J. Singh, R.C. Petter, T.A. Baillie, A. Whitty, The resurgence of covalent drugs, Nat. Rev. Drug Discov. 10 (2011) 307–317, https://doi.org/10.1038/nrd3410.
[10] G.J. Roth, N. Stanford, P.W. Majerus, Acetylation of prostaglandin synthase by aspirin, Proc. Natl. Acad. Sci. 72 (1975) 3073–3076, https://doi.org/10.1073/pnas.72.8.3073.
[11] R.M. Botting, Vane's discovery of the mechanism of action of aspirin changed our understanding of its clinical pharmacology, Pharm. Rep. 62 (2010) 518–525, https://doi.org/10.1016/s1734-1140(10)70308-x.
[12] R.M. Ward, G.L. Kearns, Proton pump inhibitors in pediatrics: mechanism of action, pharmacokinetics, pharmacogenetics, and pharmacodynamics, Paediatr. Drugs 15 (2013) 119–131, https://doi.org/10.1007/s40272-013-0012-x.
[13] A.H. Schapira, Monoamine oxidase B inhibitors for the treatment of Parkinson's disease: a review of symptomatic and potential disease-modifying effects, CNS Drugs 25 (2011) 1061–1071, https://doi.org/10.2165/11596310-000000000-00000.
[14] A.L. Maycock, R.H. Abeles, J.I. Salach, T.P. Singer, The structure of the covalent adduct formed by the interaction of 3-dimethylamino-1-propyne and the flavine of mitochondrial amine oxidase, Biochemistry 15 (1976) 114–125, https://doi.org/10.1021/bi00646a018.

[15] R. Roskoski Jr., Properties of FDA-approved small molecule protein kinase inhibitors: a 2024 update, Pharm. Res. 200 (2024) 107059, https://doi.org/10.1016/j.phrs.2024.107059.
[16] R. Roskoski Jr., Properties of FDA-approved small molecule protein kinase inhibitors: a 2025 update, Pharm. Res. 216 (2025) 107723, https://doi.org/10.1016/j.phrs.2025.107723.
[17] M.A. Lemmon, J. Schlessinger, Cell signaling by receptor tyrosine kinases, Cell 141 (2010) 1117–1134, https://doi.org/10.1016/j.cell.2010.06.011.
[18] S. Cohen, The epidermal growth factor (EGF), Cancer 51 (1983) 1787–1791, https://doi.org/10.1002/1097-0142(19830515)51:10< 1787::aid-cncr2820511004> 3.0.co;2-a.
[19] G. Carpenter, S. Cohen, Epidermal growth factor, J. Biol. Chem. 265 (1990) 7709–7712.
[20] S. Cohen, H. Ushiro, C. Stoscheck, M. Chinkers, A native 170,000 epidermal growth factor receptor-kinase complex from shed plasma membrane vesicles, J. Biol. Chem. 257 (1982) 1523–1531.
[21] S.P. Kennedy, J.F. Hastings, J.Z. Han, D.R. Croucher, The under-appreciated promiscuity of the epidermal growth factor receptor family (eCollection), Front Cell Dev. Biol. 2016 4 (2016) 88, https://doi.org/10.3389/fcell.2016.00088.
[22] R. Roskoski Jr., The ErbB/HER receptor protein-tyrosine kinases and cancer, Biochem Biophys. Res Commun. 319 (2004) 1–11, https://doi.org/10.1016/j.bbrc.2004.04.150.
[23] R. Roskoski Jr., The ErbB/HER family of protein-tyrosine kinases and cancer, Pharm. Res. 79 (2014) 34–74, https://doi.org/10.1016/j.phrs.2013.11.002.
[24] R. Roskoski Jr., ErbB/HER protein-tyrosine kinases: Structure and small molecule inhibitors, Pharm. Res 87 (2014) 42–59, https://doi.org/10.1016/j.phrs.2014.06.001.
[25] R. Roskoski Jr., Small molecule inhibitors targeting the EGFR/ErbB family of protein-tyrosine kinases in human cancers, Pharm. Res 139 (2019) 395–411, https://doi.org/10.1016/j.phrs.2018.11.014.
[26] A.L. Schechter, D.F. Stern, L. Vaidyanathan, S.J. Decker, J.A. Drebin, M.I. Greene, R.A. Weinberg, The *neu* oncogene: an erb-B-related gene encoding a 185,000-Mr tumour antigen, Nature 312 (1984) 513–516, https://doi.org/10.1038/312513a0.
[27] A. Ullrich, L. Coussens, J.S. Hayflick, T.J. Dull, A. Gray, A.W. Tam, J. Lee, Y. Yarden, T.A. Libermann, J. Schlessinger, J. Downward, E.L.V. Mayes, N. Whittle, M.D. Waterfield, P.H. Seeburg, Human epidermal growth factor receptor cDNA sequence and aberrant expression of the amplified gene in A431 epidermoid carcinoma cells, Nature 309 (1984) 418–425, https://doi.org/10.1038/309418a0.
[28] E. Tzahar, H. Waterman, X. Chen, G. Levkowitz, D. Karunagaran, S. Lavi, B. J. Ratzkin, Y. Yarden, A hierarchical network of interreceptor interactions determines signal transduction by Neu differentiation factor/neuregulin and epidermal growth factor, Mol. Cell Biol. 16 (1996) 5276–5287, https://doi.org/10.1128/MCB.16.10.5276.
[29] D. Graus-Porta, R.R. Beerli, J.M. Daly, N.E. Hynes, ErbB-2, the preferred heterodimerization partner of all ErbB receptors, is a mediator of lateral signaling, EMBO J. 16 (1997) 1647–1655, https://doi.org/10.1093/emboj/16.7.1647.
[30] R. Pinkas-Kramarski, L. Soussan, H. Waterman, G. Levkowitz, I. Alroy, L. Klapper, S. Lavi, R. Seger, B.J. Ratzkin, M. Sela, Y. Yarden, Diversification of Neu differentiation factor and epidermal growth factor signaling by combinatorial receptor interactions, EMBO J. 15 (1996) 2452–2467.
[31] D.R. Knighton, J.H. Zheng, L.F. Ten Eyck, V.A. Ashford, N.H. Xuong, S.S. Taylor, J.M. Sowadski, Crystal structure of the catalytic subunit of cyclic adenosine monophosphate-dependent protein kinase, Science 253 (1991) 407–414, https://doi.org/10.1126/science.1862342.
[32] S.S. Taylor, E. Radzio-Andzelm, T. Hunter, How do protein kinases discriminate between serine/threonine and tyrosine? Structural insights from the insulin receptor protein-tyrosine kinase, FASEB J. 9 (1995) 1255–1266, https://doi.org/10.1096/fasebj.9.13.7557015.
[33] N. Gotoh, A. Tojo, M. Hino, Y. Yazaki, M. Shibuya, A highly conserved tyrosine residue at codon 845 within the kinase domain is not required for the transforming activity of human epidermal growth factor receptor, Biochem Biophys. Res Commun. 186 (1992) 768–774, https://doi.org/10.1016/0006-291x(92)90812-y.
[34] A.P. Kornev, N.M. Haste, S.S. Taylor, L.F. Eyck, Surface comparison of active and inactive protein kinases identifies a conserved activation mechanism, Proc. Natl. Acad. Sci. 103 (2006) 17783–17788, https://doi.org/10.1073/pnas.0607656103.
[35] A.P. Kornev, S.S. Taylor, L.F. Ten Eyck, A helix scaffold for the assembly of active protein kinases, Proc. Natl. Acad. Sci. 105 (2008) 14377–14382, https://doi.org/10.1073/pnas.0807988105.
[36] R. Roskoski Jr., Cyclin-dependent protein serine/threonine kinase inhibitors as anticancer drugs, Pharm. Res. 139 (2019) 471–488, https://doi.org/10.1016/j.phrs.2018.11.035.
[37] R. Roskoski Jr., Ibrutinib inhibition of Bruton protein-tyrosine kinase (BTK) in the treatment of B cell neoplasms, Pharm. Res. 113 (2016) 395–408, https://doi.org/10.1016/j.phrs.2016.09.011.
[38] R. Roskoski Jr., The role of fibroblast growth factor receptor (FGFR) protein-tyrosine kinase inhibitors in the treatment of cancers including those of the urinary bladder, 104567, Pharm. Res. 151 (2020), https://doi.org/10.1016/j.phrs.2019.104567.
[39] R. Roskoski Jr., Janus kinase (JAK) inhibitors in the treatment of inflammatory and neoplastic diseases, Pharm. Re.s 111 (2016) 784–803, https://doi.org/10.1016/j.phrs.2016.07.038.
[40] R. Roskoski Jr., Anaplastic lymphoma kinase (ALK): structure, oncogenic activation, and pharmacological inhibition, Pharm. Res. 68 (2013) 68–94, https://doi.org/10.1016/j.phrs.2012.11.007.
[41] R. Roskoski Jr., Anaplastic lymphoma kinase (ALK) inhibitors in the treatment of ALK-driven lung cancers, Pharm. Res. 117 (2017) 343–356, https://doi.org/10.1016/j.phrs.2017.01.007.
[42] R. Roskoski Jr., The role of small molecule Kit protein-tyrosine kinase inhibitors in the treatment of neoplastic disorders, Pharm. Res. 133 (2018) 35–52, https://doi.org/10.1016/j.phrs.2018.04.020.
[43] R. Roskoski Jr., The preclinical profile of crizotinib in the treatment of non-small cell lung cancer and other neoplastic disorders, Expert Opin. Drug Dis. 8 (2013) 1165–1179, https://doi.org/10.1517/17460441.2013.813015.
[44] R. Roskoski Jr., The role of small molecule platelet-derived growth factor receptor (PDGFR) inhibitors in the treatment of neoplastic disorders, Pharm. Res. 129 (2018) 65–83, https://doi.org/10.1016/j.phrs.2018.01.021.
[45] R. Roskoski Jr, A. Sadeghi-Nejad, Role of RET protein-tyrosine kinase inhibitors in the treatment RET-driven thyroid and lung cancers, Pharm. Res. 128 (2018) 1–17, https://doi.org/10.1016/j.phrs.2017.12.021.
[46] R. Roskoski Jr., Vascular endothelial growth factor (VEGF) and VEGF receptor inhibitors in the treatment of renal cell carcinomas, Pharm. Res 120 (2017) 116–132, https://doi.org/10.1016/j.phrs.2017.03.010.
[47] R. Roskoski Jr., ROS1 protein-tyrosine kinase inhibitors in the treatment of ROS1 fusion protein-driven non-small cell lung cancers, Pharm. Res. 121 (2017) 202–212, https://doi.org/10.1016/j.phrs.2017.04.022.
[48] R. Roskoski Jr., Src protein-tyrosine kinase structure, mechanism, and small molecule inhibitors, Pharm. Res. 94 (2015) 9–25, https://doi.org/10.1016/j.phrs.2015.01.003.
[49] M.C. Frame, R. Roskoski Jr., Reference module in life sciences (Src family tyrosine kinases), Elsevier, Amsterdam, 2017, pp. 1–11, https://doi.org/10.1016/B978-0-12-809633-8.07199-5 (Src family tyrosine kinases).
[50] R. Roskoski Jr., MEK1/2 dual-specificity protein kinases: structure and regulation, Biochem Biophys. Res Commun. 417 (2012) 5–10, https://doi.org/10.1016/j.bbrc.2011.11.145.
[51] R. Roskoski Jr., Allosteric MEK1/2 inhibitors including cobimetanib and trametinib in the treatment of cutaneous melanomas, Pharm. Res 117 (2017) 20–31, https://doi.org/10.1016/j.phrs.2016.12.009.
[52] R. Roskoski Jr., ERK1/2 MAP kinases: structure, function, and regulation, Pharm. Res. 66 (2012) 105–143, https://doi.org/10.1016/j.phrs.2012.04.005, doi: 10.1016/j.phrs.2012.04.005.
[53] R. Roskoski Jr., Targeting ERK1/2 protein-serine/threonine kinases in human cancers, Pharm. Res. 142 (2019) 151–168, https://doi.org/10.1016/j.phrs.2019.03.019.
[54] R. Roskoski Jr., Cyclin-dependent protein kinase inhibitors including palbociclib as anticancer drugs, Pharm. Res. 111 (2016) 784–803, https://doi.org/10.1016/j.phrs.2016.03.012.
[55] R. Roskoski Jr., Targeting oncogenic Raf protein-serine/threonine kinases in human cancers, Pharm. Res 135 (2018) 239–258, https://doi.org/10.1016/j.phrs.2018.08.013.
[56] R. Roskoski Jr., RAF protein-serine/threonine kinases: structure and regulation, Biochem Biophys. Res. Commun. 399 (2010) 313–317, https://doi.org/10.1016/j.bbrc.2010.07.092.
[57] H.S. Meharena, P. Chang, M.M. Keshwani, K. Oruganty, A.K. Nene, N. Kannan, S. S. Taylor, A.P. Kornev, Deciphering the structural basis of eukaryotic protein kinase regulation, PLoS Biol. 11 (2013) e1001680, https://doi.org/10.1371/journal.pbio.1001680.
[58] K. Shah, Y. Liu, C. Deirmengian, K.M. Shokat, Engineering unnatural nucleotide specificity for Rous sarcoma virus tyrosine kinase to uniquely label its direct substrates, Proc. Natl. Acad. Sci. 94 (1997) 3565–3570, https://doi.org/10.1073/pnas.94.8.3565.
[59] Y. Liu, K. Shah, F. Yang, L. Witucki, K.M. Shokat, A molecular gate which controls unnatural ATP analogue recognition by the tyrosine kinase v-Src. Bioorganic, Med Chem. 6 (1998) 1219–1226, https://doi.org/10.1016/s0968-0896(98)00099-6.
[60] J. Zhou, J.A. Adams, Participation of ADP dissociation in the rate-determining step in cAMP-dependent protein kinase, Biochemistry 36 (1997) 15733–15738, https://doi.org/10.1021/bi971438n.
[61] Vetrie D., Vorechovský I., Sideras P., Holland J., Davies A., Flinter F., Hammarström L., Kinnon C., Levinsky R., Bobrow M., Edvard Smith C.I., Bentley D.R.. The gene involved in X-linked agammaglobulinaemia is a member of the src family of protein-tyrosine kinases. Nature 1993;361:226–33. doi: 10.1038/361226a0. Erratum in: Nature 1993;364:362.
[62] S. Tsukada, D.C. Saffran, D.J. Rawlings, O. Parolini, R.C. Allen, I. Klisak, R. S. Sparkes, H. Kubagawa, T. Mohandas, S. Quan, J.W. Belmont, M.D. Cooper, M. E. Conley, O.N. Witte, Deficient expression of a B cell cytoplasmic tyrosine kinase in human X-linked agammaglobulinemia, Cell 72 (1993) 279–290, https://doi.org/10.1016/0092-8674(93)90667-f.
[63] J.D. Thomas, P. Sideras, C.I. Smith, I. Vorechovský, V. Chapman, W.E. Paul, Colocalization of X-linked agammaglobulinemia and X-linked immunodeficiency genes, Science 261 (1993) 355–358.
[64] D.J. Rawlings, D.C. Saffran, S. Tsukada, D.A. Largaespada, J.C. Grimaldi, L. Cohen, R.N. Mohr, J.F. Bazan, M. Howard, N.G. Copeland, N.E. Jenkins, O. N. Witte, Mutation of unique region of Bruton's tyrosine kinase in immunodeficient XID mice, Science 261 (1993) 358–361, https://doi.org/10.1126/science.8332901.
[65] T. Helsten, M. Schwaederle, R. Kurzrock, Fibroblast growth factor receptor signaling in hereditary and neoplastic disease: biologic and clinical implications,

Cancer Metastasis Rev. 34 (2015) 479–496, https://doi.org/10.1007/s10555-015-9579-8.
[66] R. Goetz, M. Mohammadi, Exploring mechanisms of FGF signalling through the lens of structural biology, Nat. Rev. Mol. Cell Biol. 14 (2013) 166–180, https://doi.org/10.1038/nrm3528.
[67] C.M. Furdui, E.D. Lew, J. Schlessinger, K.S. Anderson, Autophosphorylation of FGFR1 kinase is mediated by a sequential and precisely ordered reaction, Mol. Cell 21 (2006) 711–717, https://doi.org/10.1016/j.molcel.2006.01.022.
[68] N. Turner, R. Grose, Fibroblast growth factor signalling: from development to cancer, Nat. Rev. Cancer 10 (2010) 116–129, https://doi.org/10.1038/nrc2780.
[69] K. Yamaoka, P. Saharinen, M. Pesu, V.E. Holt 3rd, O. Silvennoinen, J.J. O'Shea, The Janus kinases (Jaks), Genome Biol. 5 (2004) 253, https://doi.org/10.1186/gb-2004-5-12-253.
[70] X. Hu, J. Li, M. Fu, X. Zhao, W. Wang, The JAK/STAT signaling pathway: from bench to clinic, Signal Transduct. Target Ther. 6 (2021) 402, https://doi.org/10.1038/s41392-021-00791-1.
[71] R. Roskoski Jr., Deucravacitinib is an allosteric TYK2 protein kinase inhibitor FDA-approved for the treatment of psoriasis, Pharm. Res. 189 (2023) 106642, https://doi.org/10.1016/j.phrs.2022.106642.
[72] R.S. Herbst, J.V. Heymach, S.M. Lippman, Lung cancer, N. Engl. J. Med. 359 (2008) 1367–1380, https://doi.org/10.1056/NEJMra0802714.
[73] C.H. Yun, T.J. Boggon, Y. Li, M.S. Woo, H. Greulich, M. Meyerson, M.J. Eck, Structures of lung cancer-derived EGFR mutants and inhibitor complexes: mechanism of activation and insights into differential inhibitor sensitivity, Cancer Cell 11 (2007) 217–227, https://doi.org/10.1016/j.ccr.2006.12.017.
[74] G.J. Riely, D.E. Wood, D.S. Ettinger, D.L. Aisner, W. Akerley, J.R. Bauman, A. Bharat, D.S. Bruno, J.Y. Chang, L.R. Chirieac, M. DeCamp, A.P. Desai, T. J. Dilling, J. Dowell, G.A. Durm, S. Gettinger, T.E. Grotz, M.A. Gubens, A. Juloori, R.P. Lackner, M. Lanuti, J. Lin, B.W. Loo, C.M. Lovly, F. Maldonado, E. Massarelli, D. Morgensztern, T.C. Mullikin, T. Ng, D. Owen, D.H. Owen, S.P. Patel, T. Patil, P. M. Polanco, J. Riess, T.A. Shapiro, A.P. Singh, J. Stevenson, A. Tam, T. Tanvetyanon, J. Yanagawa, S.C. Yang, E. Yau, K.M. Gregory, L. Hang, Non-small cell lung cancer, Version 4.2024, NCCN clinical practice guidelines in oncology, J. Natl. Compr. Canc Netw. 22 (2024) 249–274, https://doi.org/10.6004/jnccn.2204.0023.
[75] R. Roskoski Jr., Targeted and cytotoxic inhibitors used in the treatment of lung cancers, Pharm. Res 209 (2024) 107465, https://doi.org/10.1016/j.phrs.2024.107465.
[76] M.L. Meyer, S. Peters, T.S. Mok, S. Lam, P.C. Yang, C. Aggarwal, J. Brahmer, R. Dziadziuszko, E. Felip, A. Ferris, P.M. Forde, J. Gray, L. Gros, B. Halmos, R. Herbst, P.A. Jänne, B.E. Johnson, K. Kelly, N.B. Leighl, S. Liu, I. Lowy, T. U. Marron, L. Paz-Ares, N. Rizvi, C.M. Rudin, E. Shum, R. Stahel, N. Trunova, P. A. Bunn, F.R. Hirsch, Lung cancer research and treatment: global perspectives and strategic calls to action, Ann. Oncol. 35 (2024) 1088–1104, https://doi.org/10.1016/j.annonc.2024.10.006.
[77] F. Bray, M. Laversanne, H. Sung, J. Ferlay, R.L. Siegel, I. Soerjomataram, A. Jemal, Global Cancer Statistics 2022: GLOBOCAN estimates of incidence and mortality worldwide for 36 cancers in 185 countries, CA Cancer J. Clin. 74 (2024) 229–263, https://doi.org/10.3322/caac.21834.
[78] R.L. Siegel, T.B. Kratzer, A.N. Giaquinto, H. Sung, A. Jemal, Cancer statistics, 2025, CA Cancer J. Clin. 75 (2025) 10–45, https://doi.org/10.3322/caac.21871.
[79] J.L. Wittliff, Steroid-hormone receptors in breast cancer, Cancer 53 (1984) 630–643, https://doi.org/10.1002/1097-0142(19840201)53:3+ <630::aid-cncr2820531308> 3.0.co;2-3.
[80] R. Roskoski Jr., Targeted and cytotoxic inhibitors used in the treatment of breast cancer, Pharm. Res 210 (2024) 107534, https://doi.org/10.1016/j.phrs.2024.107534.
[81] S.P. Gampenrieder, V. Castagnaviz, G. Rinnerthaler, R. Greil, Treatment landscape for patients with HER2-positive metastatic breast cancer: a review on emerging treatment options, Cancer Manag Res 12 (2020) 10615–10629, https://doi.org/10.2147/CMAR.S235121.
[82] G. von Minckwitz, Docetaxel/anthracycline combinations for breast cancer treatment, Expert Opin. Pharm. 8 (2007) 485–495, https://doi.org/10.1517/14656566.8.4.485.
[83] R. Bose, S.M. Kavuri, A.C. Searleman, W. Shen, D. Shen, D.C. Koboldt, J. Monsey, N. Goel, A.B. Aronson, S. Li, C.X. Ma, L. Ding, E.R. Mardis, M.J. Ellis, Activating HER2 mutations in HER2 gene amplification negative breast cancer. Cancer Discov 3 (2013) 224–237, https://doi.org/10.1158/2159-8290.CD-12-0349.
[84] H.C. Kluin-Nelemans, E. Hoster, O. Hermine, J. Walewski, M. Trneny, C. H. Geisler, S. Stilgenbauer, C. Thieblemont, U. Vehling-Kaiser, J.K. Doorduijn, B. Coiffier, R. Forstpointner, H. Tilly, L. Kanz, P. Feugier, M. Szymczyk, M. Hallek, S. Kremers, G. Lepeu, L. Sanhes, J.M. Zijlstra, R. Bouabdallah, P.J. Lugtenburg, M. Macro, M. Pfreundschuh, V. Procházka, F. Di Raimondo, V. Ribrag, M. Uppenkamp, M. André, W. Klapper, W. Hiddemann, M. Unterhalt, M. H. Dreyling, Treatment of older patients with mantle-cell lymphoma, N. Engl. J. Med. 367 (2012) 520–531, https://doi.org/10.1056/NEJMoa1200920.
[85] M.L. Wang, S. Rule, P. Martin, A. Goy, R. Auer, B.S. Kahl, W. Jurczak, R. H. Advani, J.E. Romaguera, M.E. Williams, J.C. Barrientos, E. Chmielowska, J. Radford, S. Stilgenbauer, M. Dreyling, W.W. Jedrzejczak, P. Johnson, S. E. Spurgeon, L. Li, L. Zhang, K. Newberry, Z. Ou, N. Cheng, B. Fang, J. McGreivy, F. Clow, J.J. Buggy, B.Y. Chang, D.M. Beaupre, L.A. Kunkel, K.A. Blum, B.T. K. Targeting, with ibrutinib in relapsed or refractory mantle-cell lymphoma, N. Engl. J. Med. 369 (2013) 507–516, https://doi.org/10.1056/NEJMoa1306220.
[86] R.A. de Claro, K.M. McGinn, N. Verdun, S.L. Lee, H.J. Chiu, H. Saber, M. E. Brower, C.J. Chang, E. Pfuma, B. Habtemariam, J. Bullock, Y. Wang, L. Nie, X. H. Chen, D.R. Lu, A. Al-Hakim, R.C. Kane, E. Kaminskas, R. Justice, A.T. Farrell, R. Pazdur, FDA approval: ibrutinib for patients with previously treated mantle cell lymphoma and previously treated chronic lymphocytic leukemia, Clin. Cancer Res. 21 (2015) 3586–3590, https://doi.org/10.1158/1078-0432.CCR-14-2225.
[87] G. Fabbri, R. Dalla-Favera, The molecular pathogenesis of chronic lymphocytic leukaemia, Nat. Rev. Cancer 16 (2016) 145–162, https://doi.org/10.1038/nrc.2016.8.
[88] A.V. Danilov, D.O. Persky, Incorporating acalabrutinib, a selective next-generation Bruton tyrosine kinase inhibitor, into clinical practice for the treatment of haematological malignancies, Br. J. Haematol. (2020), https://doi.org/10.1111/bjh.17184.
[89] Gertz M.A. Waldenström macroglobulinemia: 2025 update on diagnosis, risk stratification, and management. Am J Hematol 2025 Mar 17. doi: 10.1002/ajh.27666.
[90] Castillo J.J., Treon S.P.. Management of Waldenström macroglobulinemia in 2020. Hematology Am Soc Hematol Educ Program 2020;2020:3723379. doi: 10.1182/hematology.2020000121.
[91] A. Broccoli, M. Del Re, R. Danesi, P.L. Zinzani, Covalent Bruton tyrosine kinase inhibitors across generations: a focus on zanubrutinib, J. Cell Mol. Med. 29 (2025) e70170, https://doi.org/10.1111/jcmm.70170.
[92] S.U. Gandhy, S.J. Casak, S.L. Mushti, J. Cheng, S. Subramaniam, H. Zhao, M. Zhao, Y. Bi, G. Liu, J. Fan, O. Adeniyi, R. Charlab, D. Kufrin, M.D. Thompson, K. Jarrell, D. Auth, S.J. Lemery, R. Pazdur, P.G. Kluetz, L.A. Fashoyin-Aje, FDA approval summary: futibatinib for unresectable advanced or metastatic, chemotherapy refractory intrahepatic cholangiocarcinoma with FGFR2 fusions or other rearrangements, Clin. Cancer Res 29 (2023) 4027–4031, https://doi.org/10.1158/1078-0432.CCR-23-1042.
[93] R. Roskoski Jr., Futibatinib (Lytgobi) for cholangiocarcinoma, Trends Pharm. Sci. 44 (2023) 190–191, https://doi.org/10.1016/j.tips.2022.12.007.
[94] A.K. Gupta, T. Wang, S. Polla Ravi, M.A. Bamimore, V. Piguet, A. Tosti, Systematic review of newer agents for the management of alopecia areata in adults: Janus kinase inhibitors, biologics and phosphodiesterase-4 inhibitors. J Eur, Acad. Dermatol. Venereol. 37 (2023) 666–679, https://doi.org/10.1111/jdv.18810.
[95] I. Chim, R. Ghiya, R.D. Sinclair, S. Eisman, Novel investigational drugs for alopecia areata and future perspectives, Expert Opin. Invest. Drugs 33 (2024) 441–449, https://doi.org/10.1080/13543784.2024.2348062.
[96] M.H. Fitzhugh, J.G. Hansen, A. Jabbari, K.G. Berrebi, Pathophysiology of alopecia areata in the pediatric patient, Suppl 1, Pedia Dermatol. 42 (1) (2025) 24–30, https://doi.org/10.1111/pde.15842.
[97] T. Dainichi, M. Iwata, Y. Kaku, Alopecia areata: What's new in the diagnosis and treatment with JAK inhibitors, J. Dermatol. (2023), https://doi.org/10.1111/1346-8138.17064.
[98] T. Passeron, B. King, J. Seneschal, M. Steinhoff, A. Jabbari, M. Ohyama, D. J. Tobin, S. Randhawa, A. Winkler, J.B. Telliez, D. Martin, A. Lejeune, Inhibition of T-cell activity in alopecia areata: recent developments and new directions, Front Immunol. 14 (2023) 1243556, https://doi.org/10.3389/fimmu.2023.1243556.
[99] A.K. Gupta, S.P. Ravi, K. Vincent, W. Abramovits, LITFULO™ (Ritlecitinib) capsules: a Janus kinase 3 inhibitor for the treatment of severe alopecia areata (eCollection), Skinmed 2023 21 (2023) 434–438.
[100] A.C. Dar, K.M. Shokat, The evolution of protein kinase inhibitors from antagonists to agonists of cellular signaling, Annu Rev. Biochem. 80 (2011) 769–795, https://doi.org/10.1146/annurev-biochem-090308-173656.
[101] F. Zuccotto, E. Ardini, E. Casale, M. Angiolini, Through the "gatekeeper door": exploiting the active kinase conformation, J. Med Chem. 53 (2010) 2691–2694, https://doi.org/10.1021/jm901443h.
[102] L.K. Gavrin, E. Saiah, Approaches to discover non-ATP site inhibitors, Med. Chem. Commun. 4 (2013) 41, https://doi.org/10.1039/C2MD20180A.
[103] V. Lamba, I. Ghosh, New directions in targeting protein kinases: focusing upon true allosteric and bivalent inhibitors, Curr. Pharm. Des. 18 (2012) 2936–2945, https://doi.org/10.2174/138161212800672813.
[104] J.J. Liao, Molecular recognition of protein kinase binding pockets for design of potent and selective kinase inhibitors, J. Med. Chem. 50 (2007) 409–424, https://doi.org/10.1021/jm0608107.
[105] O.P. van Linden, A.J. Kooistra, R. Leurs, I.J. de Esch, C. de Graaf, KLIFS: a knowledge-based structural database to navigate kinase-ligand interaction space, J. Med. Chem. 57 (2014) 249–277, https://doi.org/10.1021/jm400378w.
[106] G.K. Kanev, C. de Graaf, B.A. Westerman, I.J.P. de Esch, A.J. Kooistra, KLIFS: an overhaul after the first 5 years of supporting kinase research, Nucleic Acids Res. 49 (D1) (2021) D562–D569, https://doi.org/10.1093/nar/gkaa895.
[107] R. Roskoski Jr., Orally effective FDA-approved protein kinase targeted covalent inhibitors (TCIs, Pharm. Res. 165 (2021) 105422, https://doi.org/10.1016/j.phrs.2021.105422.
[108] S.M. Abdallah, V. Hirsh, Irreversible tyrosine kinase inhibition of epidermal growth factor receptor with afatinib in *EGFR* activating mutation-positive advanced non-small-cell lung cancer, Curr. Oncol. 25 (2018) S9–S17, https://doi.org/10.3747/co.25.3732.
[109] M.R. Finlay, M. Anderton, S. Ashton, P. Ballard, P.A. Bethel, M.R. Box, R. H. Bradbury, S.J. Brown, S. Butterworth, A. Campbell, C. Chorley, N. Colclough, D.A. Cross, G.S. Currie, M. Grist, L. Hassall, G.B. Hill, D. James, M. James, P. Kemmitt, T. Klinowska, G. Lamont, S.G. Lamont, N. Martin, H.L. McFarland, M. J. Mellor, J.P. Orme, D. Perkins, P. Perkins, G. Richmond, P. Smith, R.A. Ward, M. J. Waring, D. Whittaker, S. Wells, G.L. Wrigley, Discovery of a potent and selective EGFR inhibitor (AZD9291) of both sensitizing and T790M resistance

mutations that spares the wild type form of the receptor, J. Med. Chem. 57 (2014) 8249–8267, https://doi.org/10.1021/jm500973a.
[110] P.A. Jänne, J.C. Yang, D.W. Kim, D. Planchard, Y. Ohe, S.S. Ramalingam, M. J. Ahn, S.W. Kim, W.C. Su, L. Horn, D. Haggstrom, E. Felip, J.H. Kim, P. Frewer, M. Cantarini, K.H. Brown, P.A. Dickinson, S. Ghiorghiu, M. Ranson, AZD9291 in EGFR inhibitor-resistant non-small-cell lung cancer, N. Engl. J. Med. 372 (2015) 1689–1699, https://doi.org/10.1056/NEJMoa1411817.
[111] Hochmair M. Medical treatment options for patients with epidermal growth factor receptor mutation-positive non-small cell lung cancer suffering from brain metastases and/or leptomeningeal disease. Target Oncol 2018;13:269–85. doi: 10.1007/s11523-018-0566-1. Erratum in: Target Oncol 2018;13:667. doi: 10.1007/s11523-018-0598-6.
[112] F. Solca, G. Dahl, A. Zoephel, G. Bader, M. Sanderson, C. Klein, O. Kraemer, F. Himmelsbach, E. Haaksma, G.R. Adolf, Target binding properties and cellular activity of afatinib (BIBW 2992), an irreversible ErbB family blocker, J. Pharm. Exp. Ther. 343 (2012) 342–350, https://doi.org/10.1124/jpet.112.197756.
[113] V. Modi, R.L. Dunbrack Jr., Kincore: a web resource for structural classification of protein kinases and their inhibitors, Nucleic Acids Res 50 (2022) D654–D664, https://doi.org/10.1093/nar/gkab920.
[114] R. Roskoski Jr., Classification of small molecule protein kinase inhibitors based upon the structures of their drug-enzyme complexes, Pharm. Res. 103 (2016) 26–48, https://doi.org/10.1016/j.phrs.2015.10.021.
[115] G.M. Keating, Afatinib: a review of its use in the treatment of advanced non-small cell lung cancer, Drugs 74 (2014) 207–221, https://doi.org/10.1007/s40265-013-0170-8.
[116] J.A. Engelman, K. Zejnullahu, C.M. Gale, E. Lifshits, A.J. Gonzales, T. Shimamura, F. Zhao, P.W. Vincent, G.N. Naumov, J.E. Bradner, I.W. Althaus, L. Gandhi, G. I. Shapiro, J.M. Nelson, J.V. Heymach, M. Meyerson, K.K. Wong, P.A. Jänne, PF00299804, an irreversible pan-ERBB inhibitor, is effective in lung cancer models with EGFR and ERBB2 mutations that are resistant to gefitinib, Cancer Res. 67 (2007) 11924–11932, https://doi.org/10.1158/0008-5472.CAN-07-1885.
[117] J.B. Smaill, A.J. Gonzales, J.A. Spicer, H. Lee, J.E. Reed, K. Sexton, I.W. Althaus, T. Zhu, S.L. Black, A. Blaser, W.A. Denny, P.A. Ellis, S. Fakhoury, P.J. Harvey, K. Hook, F.O. McCarthy, B.D. Palmer, F. Rivault, K. Schlosser, T. Ellis, A. M. Thompson, E. Trachet, R.T. Winters, H. Tecle, A. Bridges, Tyrosine kinase inhibitors. 20. Optimization of substituted quinazoline and pyrido[3,4-*d*] pyrimidine derivatives as orally active, irreversible inhibitors of the epidermal growth factor receptor family, J. Med. Chem. 59 (2016) 8103–8124, https://doi.org/10.1021/acs.jmedchem.6b00883.
[118] S.H. Ou, R.A. Soo, Dacomitinib in lung cancer: a "lost generation" EGFR tyrosine-kinase inhibitor from a bygone era? Drug Des. Devel Ther. 9 (2015) 5641–5653, https://doi.org/10.2147/DDDT.S52787.
[119] T.S. Mok, Y. Cheng, X. Zhou, K.H. Lee, K. Nakagawa, S. Niho, M. Lee, R. Linke, R. Rosell, J. Corral, M.R. Migliorino, A. Pluzanski, E.I. Sbar, T. Wang, J.L. White, Y.L. Wu, Improvement in overall survival in a randomized study that compared dacomitinib with gefitinib in patients with advanced non-small-cell lung cancer and *EGFR*-activating mutations, J. Clin. Oncol. 36 (2018) 2244–2250, https://doi.org/10.1200/JCO.2018.78.7994.
[120] Y. Kobayashi, T. Fujino, M. Nishino, T. Koga, M. Chiba, Y. Sesumi, S. Ohara, M. Shimoji, K. Tomizawa, T. Takemoto, T. Mitsudomi, *EGFR* T790M and C797S mutations as mechanisms of acquired resistance to dacomitinib, J. Thorac. Oncol. 13 (2018) 727–731, https://doi.org/10.1016/j.jtho.2018.01.009.
[121] J.J. Kooijman, W.E. van Riel, J. Dylus, M.B.W. Prinsen, Y. Grobben, T.J.J. de Bitter, A.M. van Doornmalen, J.J.T.M. Melis, J.C.M. Uitdehaag, Y. Narumi, Y. Kawase, J.A.D.M. de Roos, N. Willemsen-Seegers, G.J.R. Zaman, Comparative kinase and cancer cell panel profiling of kinase inhibitors approved for clinical use from 2018 to 2020, Front Oncol. 12 (2022) 953013, https://doi.org/10.3389/fonc.2022.953013.
[122] K.S. Gajiwala, J. Feng, R. Ferre, K. Ryan, O. Brodsky, S. Weinrich, J.C. Kath, A. Stewart, Insights into the aberrant activity of mutant EGFR kinase domain and drug recognition, Structure 21 (2013) 209–219, https://doi.org/10.1016/j.str.2012.11.014.
[123] K.S. Thress, C.P. Paweletz, E. Felip, B.C. Cho, D. Stetson, B. Dougherty, Z. Lai, A. Markovets, A. Vivancos, Y. Kuang, D. Ercan, S.E. Matthews, M. Cantarini, J. C. Barrett, P.A. Jänne, G.R. Oxnard, Acquired *EGFR* C797S mutation mediates resistance to AZD9291 in non-small cell lung cancer harboring *EGFR* T790M, Nat. Med. 21 (2015) 560–562, https://doi.org/10.1038/nm.3854.
[124] M. Shirley, Dacomitinib: first global approval, Drugs 78 (2018) 1947–1953, https://doi.org/10.1007/s40265-018-1028-x.
[125] D.E. Heppner, F. Wittlinger, T.S. Beyett, T. Shaurova, D.A. Urul, B. Buckley, C. D. Pham, I.K. Schaeffner, B. Yang, B.C. Ogboo, E.W. May, E.M. Schaefer, M.J. Eck, S.A. Laufer, P.A. Hershberger, Structural basis for inhibition of mutant EGFR with lazertinib (YH25448), ACS Med. Chem. Lett. 13 (2022) 1856–1863, https://doi.org/10.1021/acsmedchemlett.2c00213.
[126] K.B. Patel, D.E. Heppner, Lazertinib: breaking the mold of third-generation EGFR inhibitors, RSC Med. Chem. (2025), https://doi.org/10.1039/d4md00800f.
[127] W.S. Huang, F. Li, Y. Gong, Y. Zhang, W. Youngsaye, Y. Xu, X. Zhu, M. T. Greenfield, A. Kohlmann, P.M. Taslimi, A. Toms, S.G. Zech, T. Zhou, B. Das, H. G. Jang, M. Tugnait, Y.E. Ye, F. Gonzalvez, T.E. Baker, S. Nadworny, Y. Ning, S. D. Wardwell, S. Zhang, A.E. Gould, Y. Hu, W. Lane, R.J. Skene, H. Zou, T. Clackson, N.I. Narasimhan, V.M. Rivera, D.C. Dalgarno, W.C. Shakespeare, Discovery of mobocertinib, a potent, oral inhibitor of EGFR exon 20 insertion mutations in non-small cell lung cancer, Bioorg. Med. Chem. Lett. 80 (2023) 129084, https://doi.org/10.1016/j.bmcl.2022.129084.
[128] A. Markham, Mobocertinib: first approval, Drugs 81 (2021) 2069–2074, https://doi.org/10.1007/s40265-021-01632-9.
[129] J. Remon, C.E. Steuer, S.S. Ramalingam, E. Felip, Osimertinib and other third-generation EGFR TKI in EGFR-mutant NSCLC patients, Ann. Oncol. 29 (suppl_1) (2018) i20–i27, https://doi.org/10.1093/annonc/mdx704.
[130] Y. Yosaatmadja, S. Silva, J.M. Dickson, A.V. Patterson, J.B. Smaill, J.U. Flanagan, M.J. McKeage, C.J. Squire, Binding mode of the breakthrough inhibitor AZD9291 to epidermal growth factor receptor revealed, J. Struct. Biol. 192 (2015) 539–544, https://doi.org/10.1016/j.jsb.2015.10.018.
[131] H.R. Tsou, E.G. Overbeek-Klumpers, W.A. Hallett, M.F. Reich, M.B. Floyd, B. D. Johnson, R.S. Michalak, R. Nilakantan, C. Discafani, J. Golas, S.K. Rabindran, R. Shen, X. Shi, Y.F. Wang, J. Upeslacis, A. Wissner, Optimization of 6,7-disubstituted-4-(arylamino) quinoline-3-carbonitriles as orally active, irreversible inhibitors of human epidermal growth factor receptor-2 kinase activity, J. Med. Chem. 48 (2005) 1107–1131, https://doi.org/10.1021/jm040159c.
[132] A. Canonici, M. Gijsen, M. Mullooly, R. Bennett, N. Bouguern, K. Pedersen, N. A. O'Brien, I. Roxanis, J.L. Li, E. Bridge, R. Finn, D. Siamon, P. McGowan, M. J. Duffy, N. O'Donovan, J. Crown, A. Kong, Neratinib overcomes trastuzumab resistance in HER2 amplified breast cancer, Oncotarget 4 (2013) 1592–1605, https://doi.org/10.18632/oncotarget.1148.
[133] N. Jiang, J.J. Lin, J. Wang, B.N. Zhang, A. Li, Z.Y. Chen, S. Guo, B.B. Li, Y.Z. Duan, R.Y. Yan, H.F. Yan, X.Y. Fu, J.L. Zhou, H.M. Yang, Y. Cui, Novel treatment strategies for patients with HER2-positive breast cancer who do not benefit from current targeted therapy drugs, Exp. Ther. Med. 16 (2018) 2183–2192, https://doi.org/10.3892/etm.2018.6459.
[134] H. Singh, A.J. Walker, L. Amiri-Kordestani, J. Cheng, S. Tang, P. Balcazar, K. Barnett-Ringgold, T.R. Palmby, X. Cao, N. Zheng, Q. Liu, J. Yu, W.F. Pierce, S. R. Daniels, R. Sridhara, A. Ibrahim, P.G. Kluetz, G.M. Blumenthal, J.A. Beaver, R. Pazdur, U.S. Food and Drug administration approval: neratinib for the extended adjuvant treatment of early-stage HER2-positive breast cancer, Clin. Cancer Res. 24 (2018) 3486–3491, https://doi.org/10.1158/1078-0432.CCR-17-3628.
[135] C.H. Yun, K.E. Mengwasser, A.V. Toms, M.S. Woo, H. Greulich, K.K. Wong, M. Meyerson, M.J. Eck, The T790M mutation in EGFR kinase causes drug resistance by increasing the affinity for ATP, Proc. Natl. Acad. Sci. 105 (2008) 2070–2075, https://doi.org/10.1073/pnas.0709662105.
[136] S. Sogabe, Y. Kawakita, S. Igaki, H. Iwata, H. Miki, D.R. Cary, T. Takagi, S. Takagi, Y. Ohta, T. Ishikawa, Structure-based approach for the discovery of pyrrolo[3,2-*d*] pyrimidine-based EGFR T790M/L858R mutant inhibitors, ACS Med Chem. Lett. 4 (2012) 201–205, https://doi.org/10.1021/ml300327z.
[137] E.D. Deeks, Neratinib: First Global approval, Drugs 77 (2017) 1695–1704, https://doi.org/10.1007/s40265-017-0811-4.
[138] D.Y. Lin, A.H. Andreotti, Structure of BTK kinase domain with the second-generation inhibitors acalabrutinib and tirabrutinib, PLoS One 18 (2023) e0290872, https://doi.org/10.1371/journal.pone.0290872.
[139] T.E. Witzig, D. Inwards, Acalabrutinib for mantle cell lymphoma, Blood 133 (2019) 2570–2574, https://doi.org/10.1182/blood.2019852368.
[140] Y. Khan, S. O'Brien, Acalabrutinib and its use in treatment of chronic lymphocytic leukemia, Future Oncol. 15 (2019) 579–589, https://doi.org/10.2217/fon-2018-0637.
[141] J. Wu, M. Zhang, D. Liu, Acalabrutinib (ACP-196): a selective second-generation BTK inhibitor, J. Hematol. Oncol. 9 (2016) 21, https://doi.org/10.1186/s13045-016-0250-9.
[142] S. Paydas, Management of adverse effects/toxicity of ibrutinib, Crit. Rev. Oncol. Hematol. 136 (2019) 56–63, https://doi.org/10.1016/j.critrevonc.2019.02.001.
[143] A.T. Bender, A. Gardberg, A. Pereira, T. Johnson, Y. Wu, R. Grenningloh, J. Head, F. Morandi, P. Haselmayer, L. Liu-Bujalski, Ability of Bruton's tyrosine kinase inhibitors to sequester Y551 and prevent phosphorylation determines potency for inhibition of Fc Receptor but not B-cell receptor signaling, Mol. Pharm. 91 (2017) 208–219, https://doi.org/10.1124/mol.116.107037.
[144] M. Das, Zanubrutinib in B-cell malignancies, Lancet Oncol. 20 (2019) e470, https://doi.org/10.1016/S1470-2045(19)30523-6.
[145] Y.Y. Syed, Zanubrutinib: First approval, Drugs 80 (2020) 91–97, https://doi.org/10.1007/s40265-019-01252-4.
[146] Y. Guo, Y. Liu, N. Hu, D. Yu, C. Zhou, G. Shi, B. Zhang, M. Wei, J. Liu, L. Luo, Z. Tang, H. Song, Y. Guo, X. Liu, D. Su, S. Zhang, X. Song, X. Zhou, Y. Hong, S. Chen, Z. Cheng, S. Young, Q. Wei, H. Wang, Q. Wang, L. Lv, F. Wang, H. Xu, H. Sun, H. Xing, N. Li, W. Zhang, Z. Wang, G. Liu, Z. Sun, D. Zhou, W. Li, L. Liu, L. Wang, Z. Wang, Discovery of zanubrutinib (BGB-3111), a novel, potent, and selective covalent inhibitor of Bruton's tyrosine kinase, J. Med. Chem. 62 (2019) 7923–7940, https://doi.org/10.1021/acs.jmedchem.9b00687.
[147] A.N. Weaver, A. Jimeno, Zanubrutinib: a new BTK inhibitor for treatment of relapsed/refractory mantle cell lymphoma, in: Drugs Today, 56, Barc, 2020, pp. 531–539, https://doi.org/10.1358/dot.2020.56.8.3158047.
[148] M. Kalyukina, Y. Yosaatmadja, M.J. Middleditch, A.V. Patterson, J.B. Smaill, C. J. Squire, TAS-120 cancer target binding: defining reactivity and revealing the first fibroblast growth factor receptor1 (FGFR1) irreversible structure, ChemMedChem 14 (2019) 494–500.
[149] L. Goyal, L. Shi, L.Y. Liu, F. Fece de la Cruz, J.K. Lennerz, S. Raghavan, et al., TAS-120 overcomes resistance to ATP-competitive FGFR inhibitors in patients with FGFR2 fusion-positive intrahepatic cholangiocarcinoma, Cancer Discov. 9 (2019) 1064–1079, https://doi.org/10.1158/2159-8290.CD-19-0182.
[150] A.K. Gupta, S.P. Ravi, K. Vincent, W. Abramovits, LITFULOTM (ritlecitinib) capsules: A Janus Kinase 3 inhibitor for the treatment of severe alopecia areata, Skinmed 21 (2023) 434–438.

[151] Telliez J.B., Dowty M.E., Wang L., Jussif J., Lin T., Li L., Moy E., Balbo P., Li W., Zhao Y., Crouse K., Dickinson C., Symanowicz P., Hegen M., Banker M.E., Vincent F., Unwalla R., Liang S., Gilbert A.M., Brown M.F., Hayward M., Montgomery J., Yang X., Bauman J., Trujillo J.I., Casimiro-Garcia A., Vajdos F.F., Leung L., Geoghegan K.F., Quazi A., Xuan D., Jones L., Hett E., Wright K., Clark J.D., Thorarensen A. Discovery of a JAK3-selective inhibitor: Functional differentiation of JAK3-selective inhibition over pan-JAK or JAK1-selective inhibition. ACS Chem Biol;11:3442–3451. doi: 10.1021/acschembio.6b00677.

[152] Q. Liu, Y. Sabnis, Z. Zhao, T. Zhang, S.J. Buhrlage, L.H. Jones, N.S. Gray, Developing irreversible inhibitors of the protein kinase cysteinome, Chem. Biol. 20 (2013) 146–159, https://doi.org/10.1016/j.chembiol.2012.12.006.

[153] D.K. Simanshu, D.V. Nissley, F. McCormick, RAS proteins and their regulators in human disease, Cell 170 (2017) 17–33, https://doi.org/10.1016/j.cell.2017.06.009.

[154] J.P. O'Bryan, Pharmacological targeting of RAS: recent success with direct inhibitors, Pharm. Res 139 (2019) 503–511, https://doi.org/10.1016/j.phrs.2018.10.021.

[155] J. Timar, K. Kashofer, Molecular epidemiology and diagnostics of KRAS mutations in human cancer, Cancer Metastasis Rev. 39 (2020) 1029–1038, https://doi.org/10.1007/s10555-020-09915-5.

[156] T. Isermann, C. Sers, C.J. Der, B. Papke, KRAS inhibitors: resistance drivers and combinatorial strategies, Trends Cancer 11 (2025) 91–116, https://doi.org/10.1016/j.trecan.2024.11.009.

[157] P.A. Jackson, J.C. Widen, D.A. Harki, K.M. Brummond, Covalent modifiers: a chemical perspective on the reactivity of α,β-unsaturated carbonyls with thiols via hetero-Michael addition reactions, J. Med Chem. 60 (2017) 839–885, https://doi.org/10.1021/acs.jmedchem.6b00788.

[158] Baillie T.A. Targeted covalent inhibitors for drug design. Angew Chem Int Ed. 2016;55:13408313421. doi: 10.1002/anie.201601091.

[159] Gehringer M., Laufer S.A.. Emerging and re-emerging warheads for targeted covalent inhibitors: applications in medicinal chemistry and chemical biology. J Med Chem 2019;62:567335724. doi: 10.1021/acs.jmedchem.8b01153.

[160] L. Hillebrand, X.J. Liang, R.A.M. Serafim, M. Gehringer, Emerging and re-emerging warheads for targeted covalent inhibitors: an update, J. Med. Chem. 67 (2024) 7668–7758, https://doi.org/10.1021/acs.jmedchem.3c01825.

[161] Baillie T.A.. Approaches to mitigate the risk of serious adverse reactions in covalent drug design. Expert Opinion Drug Discov 2020;19:1313. doi: 10.1080/17460441.2021.1832079.

[162] Miseta A., Csutora P.. Relationship between the occurrence of cysteine in proteins and the complexity of organisms. Mol Biol Evol 2000;17:123231239. doi: 10.1093/oxfordjournals.molbev.a026406.

[163] Z. Zhao, P.E. Bourne, Progress with covalent small-molecule kinase inhibitors, Drug Discov. Today 23 (2018) 727–735, https://doi.org/10.1016/j.drudis.2018.01.035.

[164] Z. Zhao, P.E. Bourne, Exploring extended warheads toward developing cysteine-targeted covalent kinase inhibitors, J. Chem. Inf. Model 64 (2024) 9517–9527, https://doi.org/10.1021/acs.jcim.4c00890.

[165] G. Wang, N.J. Seidler, S. Röhm, Y. Pan, X.J. Liang, L. Haarer, B.T. Berger, S. A. Sivashanmugam, V.R. Wydra, M. Forster, S.A. Laufer, A. Chaikuad, M. Gehringer, S. Knapp, Probing the protein kinases' cysteinome by covalent fragments, e202419736, Angew. Chem. Int. Ed. Engl. 64 (2025), https://doi.org/10.1002/anie.202419736.

[166] E. Leproult, S. Barluenga, D. Moras, J.M. Wurtz, N. Winssinger, Cysteine mapping in conformationally distinct kinase nucleotide binding sites: application to the design of selective covalent inhibitors, J. Med. Chem. 54 (2011) 1347–1355, https://doi.org/10.1021/jm101396q.

[167] Roskoski R. Jr. Guidelines for preparing color figures for everyone including the colorblind. Pharmacol Res. 2017119:240–241. Erratum in: Pharmacol Res. 2019; 139:569. doi: 10.1016/j.phrs.2017.02.005.